followed first-order kinetics with $T_{1/2}$ in the human vitreous of approximately 10 days (Csaky KG, et al. *IOVS.* 2007;48:ARVO E-Abstract 4936). In contrast, Zhu et al.[33] reported that the pharmacokinetics of intravitreal bevacizumab follow a two-compartment model with initial and terminal $T_{1/2}$ of 0.5 and 6.7 days, respectively. Our half-life results in rabbits were slightly shorter ($T_{1/2} \sim 6$ days) compared with the results of Csaky et al. and Zhu et al. in humans.

In addition, Bakri et al.[19] showed in rabbits that after a 1.25-mg intravitreal injection of bevacizumab, in the treated eye, the $T_{1/2}$ in the aqueous and vitreous humors was 4.88 and 4.32 days, respectively. In contrast, in our rabbit study, $T_{1/2}$ in the vitreous after direct injection was approximately 6 days.

The differences in our results and those of these previous studies could be explained by a difference in ocular anatomy as well as detection methods for bevacizumab. Csaky et al. (*IOVS.* 2007;48:ARVO E-Abstract 4936) and Zhu et al.[33] performed their studies in humans, whereas we used rabbits. The vitreous volume of rabbits is approximately 1.5 mL, which is only one third the volume in humans. A larger vitreous volume may need a longer duration for equal distribution and therefore possibly a longer $T_{1/2}$ in the human vitreous. This notion would be in accordance with the comparison of the pharmacokinetics of triamcinolone acetonide in rabbits[36] and humans.[37]

Furthermore, although we and Bakri et al.[19] both used rabbits, the pharmacokinetic parameters in Bakri et al. differed from those in our study in that their method detected only free bevacizumab. In this study, we used the rabbit anti-human IgG (H+L) (AffiniPure; Jackson ImmunoResearch, Inc.) which has the ability to detect both the heavy and light chains of bevacizumab. Therefore, our assay had the ability to detect three possible variants of bevacizumab in vitro: fragments of the bevacizumab molecules, the entire VEGF-bevacizumab complex, and free bevacizumab.

In the retina/choroid and iris/ciliary body after intravitreal injection, bevacizumab concentration above IC_{50} was maintained for approximately 11.7 and 10.3 weeks, respectively, whereas that above 500 ng/mL was maintained for 7.7 and 6.6 weeks. A recent report regarding long-term follow-up results for intravitreal bevacizumab treatment of neovascular age-related macular degeneration has described the mean number of injections during 1 year as 3.4.[1] Thus, a single intravitreal injection of bevacizumab is active for approximately 3 months. Our results in rabbits showed bevacizumab concentration in the retina/choroid after intravitreal injection were maintained for approximately 3 months (11.7 weeks) in the effective range and were consistent with reinjection intervals in clinical situations.

Subconjunctival injection is also an effective mode of administration for intraocular neovascular diseases. In general, drug injected into subconjunctival space has two fates: direct transscleral delivery into intraocular tissues or clearance via conjunctival blood and lymphatic flow.[38–40] Since IgG has a relatively high scleral permeability and has the same molecular weight as bevacizumab, some of the bevacizumab injected into the subconjunctival space may penetrate intraocular tissues including the retina/choroid, iris/ciliary body, and vitreous via the sclera.[41,42] The bevacizumab level in the retina/choroid and iris/ciliary body was maintained above IC_{50} for 8.6 and 8.4 weeks, respectively, whereas it was maintained above 500 ng/mL for 0.3 weeks in the iris/ciliary body. The sclera consists of collagen and elastin chains that create a fiber matrix in which the pore diameter and intracellular space may determine the permeability of drugs. Negatively charged drugs have been found to have higher permeability than those with positive charges in bovine and porcine sclera.[43,44] Proteoglycans in the sclera are negatively charged,[45] which may contribute to the binding of positively charged molecules. An isoelectric point of bevacizumab has been found to be approximately 8.4.[46] Therefore, longer $T_{1/2}$ in the iris/ciliary body and retina/choroid after subconjunctival injection compared with those after intravitreal injection may sustain bevacizumab delivery into intraocular tissues due to scleral depot binding of bevacizumab to the scleral matrix.

Since the conjunctival blood vessels do not form a tight junction barrier,[47] bevacizumab can enter into the blood circulation by pinocytosis and/or convective transport through paracellular pores in the vascular endothelial layer. The Fc receptor, which binds to both albumin and the Fc portion of IgG,[48,49] was detected in the lymphatic vessels but not in the blood vessels of the conjunctiva.[50] It may be that the function of the Fc receptor in the conjunctival lymphatic vessels is to act as an efflux receptor for the efficient elimination from the conjunctival space. Residual bevacizumab, other than the bevacizumab that directly permeated the sclera and was introduced into the blood circulation, may be eliminated from the conjunctival tissue into the lymphatic vessels via convective transport with lymphatic fluid.[51]

Systemic exposure of bevacizumab when administered by intravitreal and subconjunctival injection was very similar. Bevacizumab was detected in the fellow eyes treated by intravitreal or subconjunctival injection. Bevacizumab may have been transported through the systemic circulation into the fellow eyes. In the fellow eyes treated by intravitreal injection, bevacizumab concentration in the retina/choroid was maintained above IC_{50} for 8.0 weeks.

In the case of subconjunctival injection, our data showed that most of the bevacizumab in the treated eyes was derived from the systemic circulation, and so the retinal and choroidal pharmacokinetics profile in the fellow eyes was similar to that in the treated eyes. In the fellow eyes, bevacizumab concentration in the retina/choroid was maintained above IC_{50} for 5.2 weeks. In the iris/ciliary body, a similar profile was observed, but in the fellow eye, bevacizumab was not detected at 12 weeks after injection. Of interest, corneal deposition of bevacizumab for 4 weeks after subconjunctival injection was observed by immunohistochemistry (data not shown). Therefore, subconjunctival bevacizumab may be a promising treatment, not only for neovascular diseases of the iris, retina, and choroid but also for corneal neovascularization.

In this study, we concluded that topical administration of bevacizumab by eye drops was not effective for the treatment of intraocular neovascular diseases because of poor distribution in the target tissues. These results are in accordance with data that showed that a monoclonal antibody cannot penetrate the cornea from an in vitro chamber system.[52] Since previous reports showed that topically applied bevacizumab was effective for corneal neovascularization,[28–30] further studies are needed regarding the pharmacokinetics of drugs administered to the cornea in eye drops.

There are several reports that have noted the systemic adverse effects of bevacizumab after intravitreal injection.[53–55] These adverse effects are similar to the ones reported for intravenous administration of bevacizumab for cancer treatment, such as systemic hypertension, thromboembolic diseases and death.[56,57] In addition, Shima et al.[55] found irregular vaginal bleeding as a complication in young women receiving intravitreal injection of bevacizumab. On the other hand, there have been no complications reported in previous studies of bevacizumab injected subconjunctivally at a concentration of 2.5 mg/0.1 mL,[24–27] which is twice the dose that we used in the current study. It should be noted, however, that these were small studies with a small amount of participants. Our results suggest that systemic adverse effects of bevacizumab may occur after subconjunctival injection, as well as after intravitreal or intravenous injection. Therefore, intravitreal or subconjunc-

tival bevacizumab should be used in elderly patients with choroidal or iris neovascularization. However, efficacy in the fellow eye should be expected to derive from the systemic circulation.

In conclusion, in this study we investigated the pharmacokinetics of bevacizumab in intraocular tissues and plasma by three different routes of administration. First, we found that intravitreal injection of bevacizumab was the most effective route of administration for intraocular tissue. Second, we found that both intravitreal and subconjunctival injections of bevacizumab resulted in a high concentration in plasma, and bevacizumab was distributed into the intraocular tissues in fellow eyes via systemic circulation at a level that may be effective in blocking VEGF activity. In addition, when administered by subconjunctival injection, bevacizumab was transported systemically into intraocular tissues of treated eyes at an effective level. More research is needed to define the ideal dose of bevacizumab, administration route, and intervals that will achieve the best clinical outcome possible without systemic side effects.

References

1. Bashshur ZF, Haddad ZA, Schakal A, Jaafar RF, Saab M, Noureddin BN. Intravitreal bevacizumab for treatment of neovascular age-related macular degeneration: a one-year prospective study. *Am J Ophthalmol.* 2008;145:249–256.
2. Arevalo JF, Fromow-Guerra J, Sanchez JG, et al. Primary intravitreal bevacizumab for subfoveal choroidal neovascularization in age-related macular degeneration: results of the Pan-American Collaborative Retina Study group at 12 months follow-up. *Retina.* 2008; 28:1387–1394.
3. Avila MP, Farah ME, Santos A, Duprat JP, Woodward BW, Nau J. Twelve-month short-term safety and visual acuity results from a multicentre, prospective study of epiretinal strontium-90 brachytherapy with bevacizumab for the treatment of subfoveal choroidal neovascularisation secondary to age-related macular degeneration. *Br J Ophthalmol.* 2008;93:305–309.
4. Avery RL, Pearlman J, Pieramici DJ, et al. Intravitreal bevacizumab (Avastin) in the treatment of proliferative diabetic retinopathy. *Ophthalmology.* 2006;113:1695–1705.
5. Sawada O, Kawamura H, Kakinoki M, Sawada T, Ohji M. Vascular endothelial growth factor in aqueous humor before and after intravitreal injection of bevacizumab in eyes with diabetic retinopathy. *Arch Ophthalmol.* 2007;125:1363–1366.
6. Rizzo S, Genovesi-Ebert F, Di Bartolo E, Vento A, Miniaci S, Williams G. Injection of intravitreal bevacizumab (Avastin) as a preoperative adjunct before vitrectomy surgery in the treatment of severe proliferative diabetic retinopathy (PDR). *Graefes Arch Clin Exp Ophthalmol.* 2008;246:837–842.
7. Kook D, Wolf A, Kreutzer T, et al. Long-term effect of intravitreal bevacizumab (Avastin) in patients with chronic diffuse diabetic macular edema. *Retina.* 2008;28:1053–1060.
8. Arevalo JF, Sanchez JG, Fromow-Guerra J, et al. Comparison of two doses of primary intravitreal bevacizumab (Avastin) for diffuse diabetic macular edema: results from the Pan-American Collaborative Retina Study group (PACORES) at 12-month follow-up. *Graefes Arch Clin Exp Ophthalmol.* 2009;247(6):735–43.
9. Costa RA, Jorge R, Calucci D, Melo LA Jr, Cardillo JA, Scott IU. Intravitreal bevacizumab (Avastin) for central and hemicentral retinal vein occlusions: IBeVO study. *Retina.* 2007;27:141–149.
10. Prager F, Michels S, Kriechbaum K, et al. Intravitreal bevacizumab (Avastin) for macular edema secondary to retinal vein occlusion: twelve-month results of a prospective clinical trial. *Br J Ophthalmol.* 2009;93(4):452–456.
11. Cordero Coma M, Sobrin L, Onal S, Christen W, Foster CS. Intravitreal bevacizumab for treatment of uveitic macular edema. *Ophthalmology.* 2007;114:1574–1579.
12. Ziemssen F, Deuter CM, Stuebiger N, Zierhut M. Weak transient response of chronic uveitic macular edema to intravitreal bevacizumab (Avastin). *Graefes Arch Clin Exp Ophthalmol.* 2007;245: 917–918.
13. Avery RL. Regression of retinal and iris neovascularization after intravitreal bevacizumab (Avastin) treatment. *Retina.* 2006;26: 352–354.
14. Wakabayashi T, Oshima Y, Sakaguchi H, et al. Intravitreal bevacizumab to treat iris neovascularization and neovascular glaucoma secondary to ischemic retinal diseases in 41 consecutive cases. *Ophthalmology.* 2008;115:1571–1580.
15. Mennel S, Callizo J, Schmidt JC, Meyer CH. Acute retinal pigment epithelial tear in the untreated fellow eye following repeated bevacizumab (Avastin) injections. *Acta Ophthalmol Scand.* 2007; 85:689–691.
16. Charbel Issa P, Finger RP, Holz FG, Scholl HP. Eighteen-month follow-up of intravitreal bevacizumab in type 2 idiopathic macular telangiectasia. *Br J Ophthalmol.* 2008;92:941–945.
17. Yoon YH, Kim JG, Chung H, Lee SY. Rapid progression of subclinical age-related macular degeneration in the untreated fellow eye after intravitreal bevacizumab. *Acta Ophthalmol.* Published online August 13, 2008.
18. Sawada O, Kawamura H, Kakinoki M, Ohji M. Vascular endothelial growth factor in fellow eyes of eyes injected with intravitreal bevacizumab. *Graefes Arch Clin Exp Ophthalmol.* 2008;246: 1379–1381.
19. Bakri SJ, Snyder MR, Reid JM, Pulido JS, Singh RJ. Pharmacokinetics of intravitreal bevacizumab (Avastin). *Ophthalmology.* 2007;114: 855–859.
20. Heiduschka P, Julien S, Hofmeister S, Bartz-Schmidt KU, Schraermeyer U. Bevacizumab (Avastin) does not harm retinal function after intravitreal injection as shown by electroretinography in adult mice. *Retina.* 2008;28:46–55.
21. Shahar J, Avery RL, Heilweil G, et al. Electrophysiologic and retinal penetration studies following intravitreal injection of bevacizumab (Avastin). *Retina.* 2006;26:262–269.
22. Heiduschka P, Fietz H, Hofmeister S, et al. Penetration of bevacizumab through the retina after intravitreal injection in the monkey. *Invest Ophthalmol Vis Sci.* 2007;48:2814–2823.
23. Peters S, Heiduschka P, Julien S, Bartz-Schmidt KU, Schraermeyer U. Immunohistochemical localisation of intravitreally injected bevacizumab in the anterior chamber angle, iris and ciliary body of the primate eye. *Br J Ophthalmol.* 2008;92:541–544.
24. Awadein A. Subconjunctival bevacizumab for vascularized rejected corneal grafts. *J Cataract Refract Surg.* 2007;33:1991–1993.
25. Bahar I, Kaiserman I, McAllum P, Rootman D, Slomovic A. Subconjunctival bevacizumab injection for corneal neovascularization. *Cornea.* 2008;27:142–147.
26. Bahar I, Kaiserman I, McAllum P, Rootman D, Slomovic A. Subconjunctival bevacizumab injection for corneal neovascularization in recurrent pterygium. *Curr Eye Res.* 2008;33:23–28.
27. Erdurmus M, Totan Y. Subconjunctival bevacizumab for corneal neovascularization. *Graefes Arch Clin Exp Ophthalmol.* 2007;245: 1577–1579.
28. Kim SW, Ha BJ, Kim EK, Tchah H, Kim TI. The effect of topical bevacizumab on corneal neovascularization. *Ophthalmology.* 2008;115:33–38.
29. Bock F, Konig Y, Kruse F, Baier M, Cursiefen C. Bevacizumab (Avastin) eye drops inhibit corneal neovascularization. *Graefes Arch Clin Exp Ophthalmol.* 2008;246:281–284.
30. Uy HS, Chan PS, Ang RE. Topical bevacizumab and ocular surface neovascularization in patients with Stevens-Johnson syndrome. *Cornea.* 2008;27:70–73.
31. Papathanassiou M, Theodossiadis PG, Liarakos VS, Rouvas A, Giamarellos-Bourboulis EJ, Vergados IA. Inhibition of corneal neovascularization by subconjunctival bevacizumab in an animal model. *Am J Ophthalmol.* 2008;145:424–431.
32. Kim TI, Kim SW, Kim S, Kim T, Kim EK. Inhibition of experimental corneal neovascularization by using subconjunctival injection of bevacizumab (Avastin). *Cornea.* 2008;27:349–352.
33. Zhu Q, Ziemssen F, Henke-Fahle S, et al. Vitreous levels of bevacizumab and vascular endothelial growth factor-A in patients with choroidal neovascularization. *Ophthalmology.* 2008;115:1750–1755; 1755 e1751.
34. Krohne TU, Eter N, Holz FG, Meyer CH. Intraocular pharmacokinetics of bevacizumab after a single intravitreal injection in humans. *Am J Ophthalmol.* 2008;146:508–512.

35. Wang Y, Fei D, Vanderlaan M, Song A. Biological activity of bevacizumab, a humanized anti-VEGF antibody in vitro. *Angiogenesis.* 2004;7:335–345.
36. Chin HS, Park TS, Moon YS, Oh JH. Difference in clearance of intravitreal triamcinolone acetonide between vitrectomized and nonvitrectomized eyes. *Retina.* 2005;25:556–560.
37. Beer PM, Bakri SJ, Singh RJ, Liu W, Peters GB 3rd, Miller M. Intraocular concentration and pharmacokinetics of triamcinolone acetonide after a single intravitreal injection. *Ophthalmology.* 2003;110:681–686.
38. Robinson MR, Lee SS, Kim H, et al. A rabbit model for assessing the ocular barriers to the transscleral delivery of triamcinolone acetonide. *Exp Eye Res.* 2006;82:479–487.
39. Ranta VP, Urtti A. Transscleral drug delivery to the posterior eye: prospects of pharmacokinetic modeling. *Adv Drug Deliv Rev.* 2006;58:1164–1181.
40. Amrite AC, Edelhauser HF, Kompella UB. Modeling of corneal and retinal pharmacokinetics after periocular drug administration. *Invest Ophthalmol Vis Sci.* 2008;49:320–332.
41. Ambati J, Canakis CS, Miller JW, et al. Diffusion of high molecular weight compounds through sclera. *Invest Ophthalmol Vis Sci.* 2000;41:1181–1185.
42. Ambati J, Gragoudas ES, Miller JW, et al. Transscleral delivery of bioactive protein to the choroid and retina. *Invest Ophthalmol Vis Sci.* 2000;41:1186–1191.
43. Maurice DM, Polgar J. Diffusion across the sclera. *Exp Eye Res.* 1977;25:577–582.
44. Cheruvu NP, Kompella UB. Bovine and porcine transscleral solute transport: influence of lipophilicity and the choroid-Bruch's layer. *Invest Ophthalmol Vis Sci.* 2006;47:4513–4522.
45. Dunlevy JR, Rada JA. Interaction of lumican with aggrecan in the aging human sclera. *Invest Ophthalmol Vis Sci.* 2004;45:3849–3856.
46. Vlckova M, Kalman F, Schwarz MA. Pharmaceutical applications of isoelectric focusing on microchip with imaged UV detection. *J Chromatogr A.* 2008;1181:145–152.
47. Raviola G. Conjunctival and episcleral blood vessels are permeable to blood-borne horseradish peroxidase. *Invest Ophthalmol Vis Sci.* 1983;24:725–736.
48. Wani MA, Haynes LD, Kim J, et al. Familial hypercatabolic hypoproteinemia caused by deficiency of the neonatal Fc receptor, FcRn, due to a mutant beta2-microglobulin gene. *Proc Natl Acad Sci U S A.* 2006;103:5084–5089.
49. Burmeister WP, Huber AH, Bjorkman PJ. Crystal structure of the complex of rat neonatal Fc receptor with Fc. *Nature.* 1994;372:379–383.
50. Kim H, Fariss RN, Zhang C, Robinson SB, Thill M, Csaky KG. Mapping of the neonatal Fc receptor in the rodent eye. *Invest Ophthalmol Vis Sci.* 2008;49:2025–2029.
51. Lobo ED, Hansen RJ, Balthasar JP. Antibody pharmacokinetics and pharmacodynamics. *J Pharm Sci.* 2004;93:2645–2668.
52. Brereton HM, Taylor SD, Farrall A, et al. Influence of format on in vitro penetration of antibody fragments through porcine cornea. *Br J Ophthalmol.* 2005;89:1205–1209.
53. Fung AE, Rosenfeld PJ, Reichel E. The International Intravitreal Bevacizumab Safety Survey: using the internet to assess drug safety worldwide. *Br J Ophthalmol.* 2006;90:1344–1349.
54. Wu L, Martinez-Castellanos MA, Quiroz-Mercado H, et al. Twelve-month safety of intravitreal injections of bevacizumab (Avastin®): results of the Pan-American Collaborative Retina Study group (PACORES). *Graefes Arch Clin Exp Ophthalmol.* 2008;246:81–87.
55. Shima C, Sakaguchi H, Gomi F, et al. Complications in patients after intravitreal injection of bevacizumab. *Acta Ophthalmol.* 2008;86:372–376.
56. Hurwitz H, Fehrenbacher L, Novotny W, et al. Bevacizumab plus irinotecan, fluorouracil, and leucovorin for metastatic colorectal cancer. *N Engl J Med.* 2004;350:2335–2342.
57. Ratner M. Genentech discloses safety concerns over Avastin. *Nat Biotechnol.* 2004;22:1198.

Neuroprotective Effects of Angiotensin II Type 1 Receptor Blocker in a Rat Model of Chronic Glaucoma

Hongwei Yang,[1,2] *Kazuyuki Hirooka,*[1] *Kouki Fukuda,*[1] *and Fumio Shiraga*[1]

Purpose. To investigate the neuroprotective effect of candesartan, an angiotensin II type 1 receptor (AT1-R) blocker, against the neurotoxicity of the retinal ganglion cells (RGCs) in an animal model of glaucoma.

Methods. Cauterization of three episcleral vessels in rats was used to create chronically elevated intraocular pressure (IOP) in one eye. Rats were then treated orally with candesartan (1 mg/kg/d). At 10 weeks, immunohistochemistry was used for quantification of RGC survival and examination of retinal localization of AT1-R.

Results. Compared with the contralateral control eyes, there was a consistently elevated IOP of approximately 2.5-fold during the experimental period. At the end of the 10-week candesartan treatment, there were no changes noted for the blood pressure. Compared with the contralateral control eyes that had normal IOP, the RGC survival rate in the central retina of eyes with the chronic, elevated IOP was 46.5% ± 19.4% (mean ± SD) in the untreated animals and 84.2% ± 4.9% in the candesartan-treated animals ($P < 0.05$; unpaired *t*-test). In the retina of the normal IOP rat eyes, retinal vessels were positive for AT1-R. After 10 weeks of IOP elevation, immunohistochemical analysis of the retina indicated there were many AT1-R-positive RGCs in the candesartan-treated rat, whereas there was an apparent AT1-R decrease in the vehicle-treated rats.

Conclusions. In the rat chronic glaucoma model, continuous pharmacologic treatment using candesartan results in significant neuroprotection against RGC loss. (*Invest Ophthalmol Vis Sci.* 2009;50:5800-5804) DOI:10.1167/iovs.09-3678

Primary open-angle glaucoma, which is one of the leading causes of vision loss in the world, is an optic neuropathy that is associated with elevated intraocular pressure (IOP). Current glaucoma treatments are based on attempts to lower elevated IOP to slow or stop the progressive loss of the visual field that occurs as a result of optic nerve degeneration and the subsequent loss of retinal ganglion cells (RGCs). However, glaucomatous damage progresses in many of these cases despite adequate control of the IOP.[1] Consequently, many investigators are trying to find a therapeutic modality that not only stabilizes the IOP at a lower level but that can prevent the death of RGCs or even lead to RGC regeneration.[2,3]

The renin-angiotensin system (RAS) plays an important part in the control of blood pressure and electrolyte homeostasis. Recent evidence suggests that in addition to the circulating RAS, there is tissue or local RAS in the vasculature, adrenal gland, kidney, brain, testis, and ovary that also may have a role in the overall control.[4-6] Many of the known RAS components have been identified in the human eye.[4,7-9] Angiotensinogen is an obligatory component for the eventual production of angiotensin II. Angiotensin I and angiotensin II are generated within the circulation by a sequential cleavage of the liver-derived angiotensinogen. Renin, which is synthesized in the kidney, cleaves this substrate, leading to the formation of angiotensin I. Angiotensin-converting enzyme (ACE) converts angiotensin I to angiotensin II. Angiotensin II is the effector molecule of the system and has two cognate receptors that are designated as angiotensin II type 1 and type 2 receptors (AT1-R and AT2-R, respectively).[10,11] Because AT1-R mediates the major functions of angiotensin II, its antagonists are widely used to treat patients with hypertension and cardiovascular diseases. Emerging evidence obtained when using the experimental cerebral ischemia model has suggested that peripherally administered AT1-R blockers (ARBs) can cross the blood-brain barrier and interact with AT1-R, thereby reducing the infarct volume.[12-14] Recently, ARBs have also been proven to attenuate inflammatory and oxidative stress in the brain[15,16] and retina.[17,18]

The long-term use of ACE inhibitors, which are widely used as antihypertensive drugs, are believed to have a favorable effect on the visual fields in patients with normal-tension glaucoma.[19] Angiotensin II receptor gene polymorphisms have been found in humans, and these may be associated with the risk for glaucoma.[20] The purpose of the present study was to investigate the effects of candesartan along with the role of ARBs in RGC degeneration in an animal model of glaucoma.

Materials and Methods

Animals

Female Sprague-Dawley rats (Charles River Japan, Yokohama, Japan), weighing 180 to 210 g each, were housed in a standard animal room under a 12-hour light/12-hour dark cycle with free access to food and water. All surgical procedures were performed under general anesthesia that used intraperitoneal injections of pentobarbital (40-50 mg/kg Nembutal; Abbott, Abbott Park, IL). Animal care and all experiments were conducted under the approved standard guidelines for animal experimentation of the Kagawa University Faculty of Medicine and adhered to the ARVO Statement for the Use of Animals in Ophthalmic and Vision Research. Two groups of rats that had unilateral elevated IOP were followed up for 10 weeks. The rats in the first group did not receive any treatments for their elevated IOP, whereas rats in the second group underwent 10 weeks of candesartan treatment (1 mg/kg/d; a gift from Takeda Pharmaceutical Co., Ltd., Osaka, Japan), with the initial dose administered on the first day of IOP elevation. Candesartan or water was orally administered to animals on a daily basis via the use of feeding needles.

From the [1]Department of Ophthalmology, Kagawa University Faculty of Medicine, Kagawa, Japan; and the [2]Department of Ophthalmology, Shengjing Affiliated Hospital, China Medical University, Shenyang, China.

Supported by a Grant-in-Aid for Scientific Research from The Ministry of Education, Culture, Sports, Science, and Technology of Japan (20592078).

Submitted for publication March 6, 2009; revised May 22 and June 9, 2009; accepted September 4, 2009.

Disclosure: **H. Yang**, None; **K. Hirooka**, None; **K. Fukuda**, None; **F. Shiraga**, None

The publication costs of this article were defrayed in part by page charge payment. This article must therefore be marked "*advertisement*" in accordance with 18 U.S.C. §1734 solely to indicate this fact.

Corresponding author: Kazuyuki Hirooka, Department of Ophthalmology, Kagawa University Faculty of Medicine, 1750-1 Ikenobe, Miki, Kagawa 761-0793, Japan; kazuyk@med.kagawa-u.ac.jp.

Chronic Elevated IOP Rat Model

We performed cauterization of three episcleral vessels in six rats to unilaterally create the chronic elevated IOP conditions. The contralateral eye served as the comparative control. Incision of the conjunctiva at the equator exposed 3 of the 4 to 5 major trunks that are formed by the limbal-derived veins. Each vessel was then lifted with a small muscle hook and cauterized by direct application of ophthalmic cautery (Tagawa, Tokyo, Japan) against the muscle hook. Successful cauterization was defined as an immediate retraction and subsequent absence of bleeding at the cauterized end of the vessels. The eyes were dressed with 0.3% ofloxacin ophthalmic ointment (Santen, Osaka, Japan).

IOP and BP Measurements

IOP was measured three times in the anesthetized rat using a handheld electronic tonometer (TonoPen XL; Bio-Rad, Glendale, CA), with the mean value used for the analysis. Bilateral IOP measurements were performed within 3 hours and 1 week of the surgery to confirm the unilateral, moderately elevated IOP. Thereafter, IOP was measured weekly.

Systolic blood pressure (SBP) and diastolic blood pressure (DBP) were measured weekly in unanesthetized rats using the tail-cuff method (BP-98A; Softron Co., Tokyo, Japan).

Retrograde Labeling of Retinal Ganglion Cells

At 7 days before kill, fluorescent dye (Fast Blue; Polysciences Inc., Warrington, PA) was injected bilaterally into the superior colliculi of anesthetized rats. The skull was exposed and kept dry and clean. After identifying and marking the bregma, a small window was drilled in the scalp in both the right and the left hemispheres. The windows were drilled to a depth of 3.6 mm from the surface of the skull, located 6.8 mm behind the bregma on the anteroposterior axis and 1.5 mm lateral to the midline. Using a Hamilton syringe, 1.5 μL of 3% fluorescent dye (Fast Blue; Polysciences Inc.) was slowly injected into the bilateral superior colliculi. After suturing the skin over the wound, antibiotic ointment was applied.

Tissue Preparation and Assessment of RGC Survival

Animals were killed by an overdose of pentobarbital (Nembutal) at 1 week after the fluorescent dye (Fast Blue; Polysciences Inc.) application. Whole flat-mounted retinas were then assayed for retinal ganglion cell density. Rat eyes were enucleated and fixed in 4% paraformaldehyde for 10 hours at room temperature. After removal of the anterior segments, the resultant posterior eyecups were left in place. Subsequently, four radial cuts were made in the periphery of the eyecup, with the retina then carefully separated from the retinal pigment epithelium. To prepare the flat mounts, the retina was dissociated from the underlying structures, flattened by making four radial cuts, and then spread on a gelatin-coated glass slide. Labeled RGCs were visualized under a fluorescence microscope (BX-51/DP70; Olympus, Tokyo, Japan) by using a filter set (excitation filter, 330–385 nm; barrier filter, 420 nm; WU; Olympus). Fluorescence-labeled RGCs were counted in 12 microscopic fields of retinal tissue from two regions in each quadrant at two different eccentricities, 1 mm (central) and 4 mm (peripheral) away from the optic disc.[21,22] Imaging software (Image-Pro Plus, version 4.0; Media Cybernetics, Bethesda, MD) was used to count approximately 15% to 20% of the total number of RGCs in each eye. Cell counts were conducted by the same person in a masked fashion, with the identity of the original retinas unknown to the investigator until completion of the cell counts from all the different groups. Changes in the densities of the RGCs were expressed as the RGC survival percentage, which was based on the comparison between the surgical and contralateral control eyes. The specimens that were compared came from different retinal regions of the same animal.

Immunohistochemistry

At 3 or 10 weeks after the initial elevation of the IOP, rats were anesthetized by intraperitoneal injection of pentobarbital and then perfused intracardially with phosphate-buffered saline (PBS). Animals were subsequently perfused with 4% paraformaldehyde in PBS. Retinal sections were rinsed in 100% ethanol twice for 5 minutes each, followed by a separate 95% ethanol and 90% ethanol rinse for 3 minutes The sections were then washed using PBS, pH 7.4, three times for 10 minutes each, followed by treatment with 0.3% Triton-X-100 in PBS, at pH 7.4, for 1 hour. After further washing three times for 10 minutes each with PBS at pH 7.4, sections were blocked in 3% normal horse serum and 1% bovine serum albumin (BSA) in PBS for 1 hour to reduce the nonspecific labeling. Tissues were incubated overnight at 4°C with primary antibodies in PBS containing 0.5% Triton X-100, 5% normal horse serum, and 1% BSA. Primary antibody was diluted as follows: rabbit polyclonal antibody against human AT1-R (Santa Cruz Biotechnology, Santa Cruz, CA) 1:100. Control sections were prepared by omitting both the primary antibody and the rabbit IgG (1:1000; Vector Laboratories Inc., Burlingame, CA) in PBS containing 0.5% Triton X-100, 5% normal horse serum, and 1% BSA overnight at 4°C. After washing in PBS for 50 minutes, tissues were immersed in the alkaline phosphatase (AP; Vectastain ABC-AP Kit; Vector Laboratories Inc.) for 30 minutes at room temperature, washed in PBS for 15 minutes, and processed using the avidin-biotin complex reagent (ABC-Reagent; Vectastain ABC-AP Kit; Vector Laboratories Inc.) for 1 hour at room temperature. Images were acquired using 40× objective lenses (DXM 1200; Nikon, Tokyo, Japan). Graphics editing software (PhotoShop version 5.0; Adobe, San Jose, CA) was used to adjust the brightness and contrast of the images.

Statistical Analysis

Statistical analysis was performed (SPSS for Windows; SPSS Inc., Chicago, IL). A paired *t*-test was used to determine the statistical significance of the BP measurements. An independent Student's *t*-test was used to compare the RGC survival rate and IOP measurements. $P < 0.05$ was considered statistically significant. All statistical values are presented as the mean ± SD.

Results

Intraocular Pressure and Blood Pressure

There was no significant difference noted between the baseline IOP values of vehicle- and candesartan-treated rats. Elevated IOP was observed over the 10-week experimental period in all eyes that underwent the three-vessel cauterization (Fig. 1). Three hours after the surgery, IOP was elevated to approximately 26 mm Hg (range, 23.7–30.3 mm Hg), and it was consistently elevated approximately 2.5-fold compared with the contralateral control eyes. In both groups, the elevated IOP was significantly higher than in contralateral control eyes. The elevation in the IOP was essentially the same between the candesartan-treated and the nontreated animals. Our success rate was 6 of 8 animals. Animals in which elevated IOP were not maintained for more than 2 weeks were excluded from the subjects.

The changes in the SBP and DBP are shown in Figure 2. Treatment with vehicle did not affect either the SBP or the DBP at week 10 in the rats (118.8 ± 6.9 mm Hg and 93.1 ± 6.4 mm Hg, respectively). Furthermore, there were no changes seen in the SBP and DBP in the rats at 10 weeks after the candesartan treatment (113.1 ± 6.1 mm Hg and 87.9 ± 5.9 mm Hg, respectively).

Effect of Candesartan on RGC Survival

Figure 3A shows representative results of the RGC labeling in both the vehicle- and the candesartan-treated rat. Compared

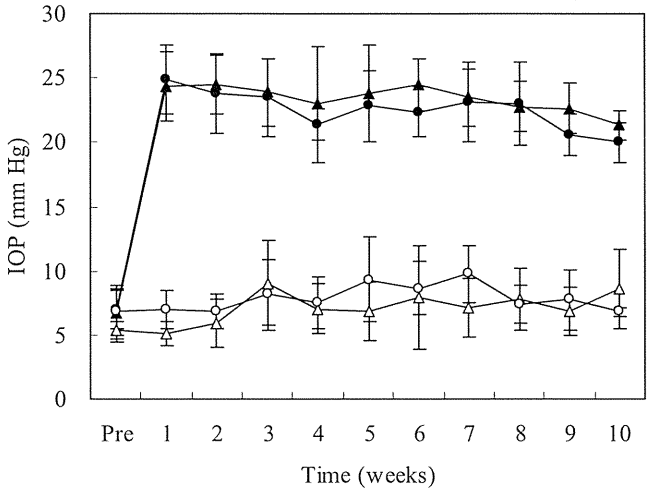

FIGURE 1. Elevated IOP in rat eyes that underwent unilateral cauterization of three episcleral vessels (Operated) compared with the opposite eye (Control). *Filled triangles*: operated, vehicle. *Filled circles*: operated, candesartan. *Open triangles*: control, vehicle. *Open circles*: control, candesartan. During the 10-week experimental period, one group of animals was not treated pharmacologically (*triangles*), whereas the other group was treated with candesartan (*circles*). All values are mean ± SD (n = 6).

with the vehicle-treated rat, RGC death seemed to be mild in the candesartan-treated rat. RGC survival rates in the central retinas of the eyes with elevated IOP were 46.5% ± 19.4% (mean ± SD) in the vehicle-treated group and 84.2% ± 5.0% in the candesartan-treated group (P = 0.02; Fig. 3B). In the peripheral retina, RGC survival rates in the eyes with elevated IOP were 52.3% ± 21.8% in the vehicle-treated group and 82.5% ± 2.4% in the candesartan-treated group (P = 0.004; Fig. 3B).

Immunohistochemistry

In the retinas of rat eyes with normal IOP, AT1-R immunoreactivity was detected on the endothelial cells of the inner retinal vessels (Fig. 4A). In the retinas of rat eyes with chronic elevated IOP, immunohistochemical analysis indicated there were many AT1-R–positive cells within the ganglion cell layer in the candesartan-treated rat, though this number was apparently decreased in the vehicle-treated rat (Figs. 4B, C). However, immunohistochemical analysis at 3 weeks after the initial elevation of IOP showed there were many AT1-R–positive cells within the retinal ganglion cell layer in the vehicle-treated rat (Fig. 4D).

Discussion

The present study demonstrates for the first time that AT1-R upregulation is associated with chronic elevated IOP in the rat model of glaucoma and that the AT1-R signaling blockade of candesartan effectively prevents retinal neuronal death. Candesartan (1 mg/kg/d) has neuroprotective effects against cerebral ischemia in spontaneously hypertensive rats.[23] In animals pretreated with 0.1 or 1 mg/kg candesartan, only 1 mg/kg candesartan reduced ischemic damage to the retina against retinal ischemia-reperfusion injury in the rat retina (KF, KH, et al., unpublished data, 2009). Therefore, the 1-mg/kg/d dose used in this study was selected.

Oral administration of the ARB losartan reduced the IOP in human subjects with both normal tension and glaucoma.[24] Hasizume et al.[20] have recently shown that candesartan causes a decrease in IOP, with an IOP reduction noted for 5 hours after drug administration in healthy subjects. The total outflow facility increased significantly in all subjects, with a decrease in the SBP noted only in patients with hypertension.[24] These results suggest that the mechanism is not mediated by a decrease in blood pressure but, rather, is more specific. These findings confirm the role of the RAS in the regulation of IOP.[24] Because candesartan treatment was performed before elevation of the IOP, we were unable to compare the IOP before and after its oral administration in this study. However, given that all the animals had cautery-induced IOP elevation, we compared the animals that were not treated pharmacologically with those that did receive candesartan and determined there was no significant difference between the two groups. Thus, we concluded that candesartan treatment provides a neuroprotective effect that is independent of IOP reduction.

IOP in the control eyes was lower than has been previously reported by other investigators (11.6–13.2 mm Hg).[21,25] This might have been due to differences associated with the anesthetic used in the present study. Anesthetics can affect IOP, and this effect can change over time, depending on the level of anesthesia present.[26,27] The most commonly used device for measuring IOP in rats is the TonoPen electronic tonometer (Reichert, Depew, NY).[21,25] Recent reports have shown the TonoLab device (Colonial Medical Supply, Franconia, NH) to be more effective than the TonoPen when measuring IOP in rats.[28,29] Moore et al.[30] have shown that there is a high correlation between the results obtained when using a TonoPen and those obtained by directly measuring the rat eye (r = 0.94–0.98). They also have reported the repeatability and consistency of IOP measurements when using the TonoPen.[30] In our study, the coefficient of variation in measuring IOP with TonoPen was 8.5%.

In the present study, we found that the 1 mg/kg/d candesartan treatment in normal rats did not affect either the SBP or the DBP. Although our results are similar to those of another study that found there was no SBP decrease from baseline after the same dose of candesartan was administered in adult and old rats, a second study has shown that a higher dose (10 mg/kg/d) of candesartan caused a significant decrease in the SBP.[31] However, since a 1-mg/kg/d candesartan dose has been shown to reduce BP in spontaneously hypertensive rats,[23] it may be that the 1-mg/kg/d candesartan dose level affects only hypertensive rats.

Kurihara et al.[32] recently reported that intense inflammation caused local upregulation of angiotensin II expression and disturbed visual function by electroretinography. The RAS polymorphisms that exist for the angiotensin II receptor gene may be a major genetic risk factor for the development or progression of glaucoma in the Japanese population.[20] Angiotensin II activates the NADPH-dependent oxidase complex, which serves as a major source of superoxide and is upregulated in several pathologic conditions associated with oxidative stress.[33,34] Given that oxidative stress induces apoptosis in neurons,[35] hydrostatic pressure-induced oxidative stress could

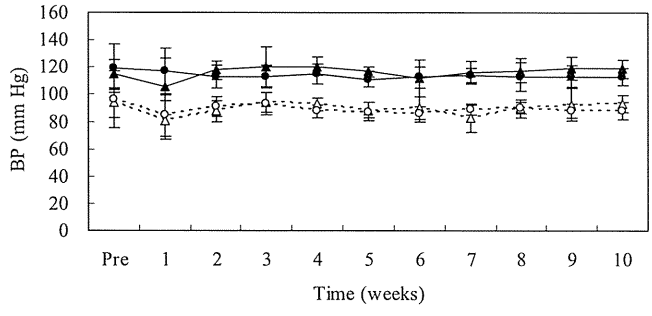

FIGURE 2. Systolic (*solid line*) and diastolic (*dotted line*) blood pressure (BP) measurements after oral administration of candesartan (*circles*) or vehicle (*triangles*). All values are mean ± SD (n = 6).

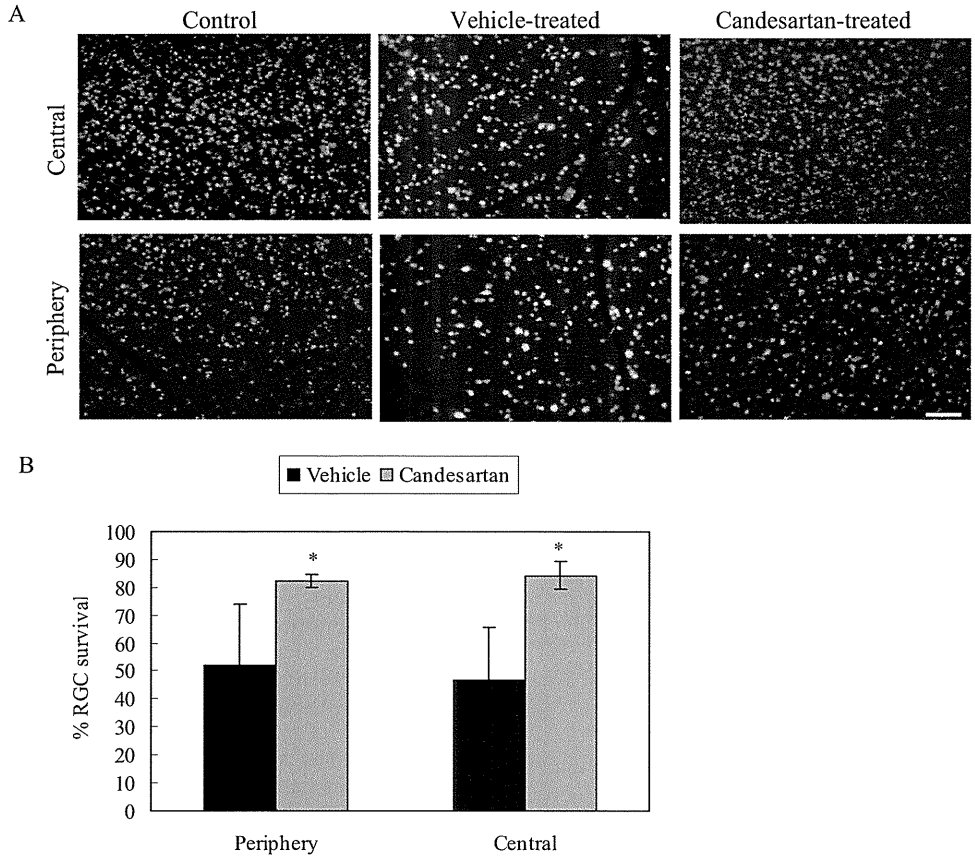

FIGURE 3. Survival of RGCs at 10 weeks in rat eyes with chronic elevated IOP. (**A**) Retrograde labeling of the RGCs in eyes with normal IOP and in eyes with elevated IOP at 10 weeks after administration of candesartan or vehicle. Micrographs in the central and peripheral areas were taken approximately 1 and 4 mm from the optic nerve head, respectively. Scale bar, 20 μm. (**B**) RGCs were counted in the central and peripheral areas at approximately 1 and 4 mm from the optic nerve head, respectively. The graph depicts the mean ± SD of six animals treated with candesartan and six animals treated with vehicle. A significant difference in the RGC survival rate in eyes with elevated IOP that were treated with candesartan and vehicle was evident between the central ($P = 0.02$) and peripheral ($P = 0.004$) areas. $^*P < 0.05$

very well be the mechanism responsible for the similar pressure-induced apoptosis seen in animal models[36,37] and in glaucoma patients with high IOP.[38] In the present study, we demonstrated that the AT1-R level increased in the ganglion cell layer in candesartan-treated rats. In vehicle-treated rats, however, there was a decrease in the AT1-R–positive RGCs in the retina 10 weeks after the elevation of IOP compared with that seen in the candesartan-treated rat. Vehicle-treated rats were

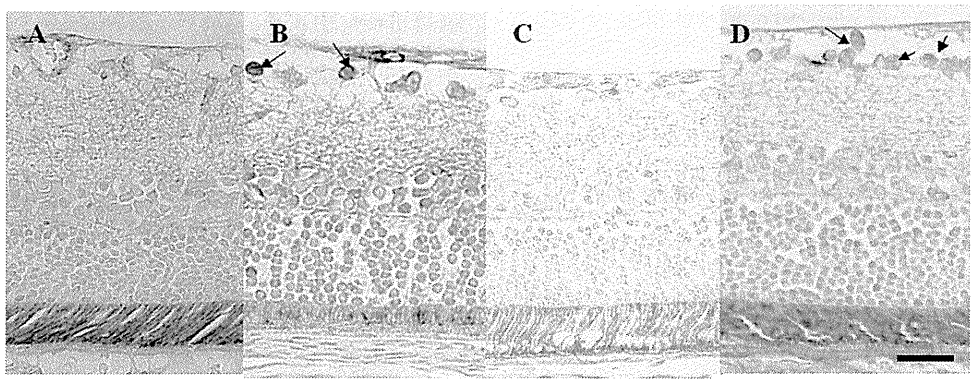

FIGURE 4. Immunohistochemical staining of the ATI-R expression in the retina. Retinal sections from normal animals (**A**) and from animals with chronic elevated IOP that were administered candesartan over a 10-week period (**B**) or vehicle over a 10-week (**C**) or a 3-week period (**D**). An increase in the AT1-R–positive RGCs (*arrow*) was noted for the candesartan-treated rats at 10 weeks and vehicle-treated rats at 3 weeks, compared with the normal and vehicle-treated rats at 10 weeks. Scale bar, 25 μm.

also found to have many AT1-R-positive RGCs in the retina 3 weeks after IOP elevation (i.e., a few weeks before the beginning of cell death). Thus, increases in the AT1-R-positive RGCs occur when IOP is chronically elevated. Treatment with candesartan effectively prevented cell death.

In conclusion, the current data suggest that candesartan does indeed have a therapeutic effect in this animal model of glaucoma. Because ARBs are safely and widely used to treat hypertension, clinical administration of candesartan for the purpose of pharmacologic neuroprotection may be a new and beneficial therapy that can be used in patients with glaucoma.

References

1. Brubaker RF. Delayed functional loss in glaucoma: LII Edward Jackson Memorial Lecture. *Am J Ophthalmol.* 1996;121:473–483.
2. Osborne NN, Chidlow G, Nash MS, Wood JP. The potential of neuroprotection in glaucoma treatment. *Curr Opin Ophthalmol.* 1999;10:82–92.
3. Chierzi S, Fawcett JW. Regeneration in the mammalian optic nerve. *Restor Neurol Neurosci.* 2001;19:109–118.
4. Danser AH, Derkx FH, Admiraal PJ, Deinum J, de Jong PT, Schalekamp MA. Angiotensin levels in the eye. *Invest Ophthalmol Vis Sci.* 1994;35:1008–1018.
5. Deschepper CF, Mellon SH, Cumin F, Baxter JD, Ganong WF. Analysis by immunocytochemistry and in situ hybridization of retina and its mRNA in kidney, testis, adrenal, and pituitary of the rat. *Proc Natl Acad Sci USA.* 1986;83:7552–7556.
6. Derkx FH, Alberda AT, Zeilmaker GH, Schalekamp MA. High concentrations of immunoreactive renin, protein and enzymatically-active renin in human ovarian follicular fluid. *Br J Obstet Gynaecol.* 1987;94:4–9.
7. Sramek SJ, Wallow IH, Tewksbury DA, Brandt CR, Poulsen GL. An ocular renin-angiotensin system; immunohistochemistry of angiotensinogen. *Invest Ophthalmol Vis Sci.* 1992;33:1627–1632.
8. Wagner J, Jan Danser AH, Derkx FH, et al. Demonstration of renin mRNA, angiotensin mRNA, and angiotensin converting enzyme mRNA expression in the human eye: evidence for an intraocular renin-angiotensin system. *Br J Ophthalmol.* 1996;80:159–163.
9. Savaskan E, Löffler KU, Meier F, Müller-Spahn F, Flammer J, Meyer P. Immunohistochemical localization of angiotensin-converting enzyme, angiotensin II and AT1 receptor in human ocular tissue. *Ophthalmic Res.* 2004;36:312–320.
10. de Gasparo M, Catt KJ, Inagami T, Wright JW, Unger T. International union of pharmacology, XXIII: the angiotensin II receptors. *Pharmacol Rev.* 2000;52:415–472.
11. Murphy TJ, Alexander RW, Griendling KK, Runge MS. Bernstein KE. Isolation of a cDNA encoding the vascular type-1 angiotensin II receptor. *Nature.* 1991;351:233–236.
12. Dai WJ, Funk A, Herdegen T, Unger T, Culman J. Blockade of central angiotensin AT(1) receptors improves neurological outcome and reduces expression of AP-1 transcription factors after focal brain ischemia in rats. *Stroke.* 1999;30:2391–2398.
13. Nishimura Y, Ito T, Saavedra JM. Angiotensin II AT(1) blockade normalizes cerebrovascular autoregulation and reduces cerebral ischemia in spontaneously hypertensive rats. *Stroke.* 2000;31:2478–2486.
14. Yamakawa H, Jezova M, Ando A, Saavedra JM. Normalization of endothelial and inducible nitric oxide synthase expression in brain microvessels of spontaneously hypertensive rats by angiotensin II AT1 receptor inhibition. *J Cereb Blood Flow Metab.* 2003;23:371–380.
15. Ando H, Zhou J, Macova M, Imboden H, Saavedra JM. Angiotensin II AT1 receptor blockade reverses pathological hypertrophy and inflammation in brain microvessels of spontaneously hypertensive rats. *Stroke.* 2004;35:1726–1731.
16. Zhou J, Ando H, Macova M, Dou J, Saavedra JM. Angiotensin II AT1 receptor blockade abolishes brain microvascular inflammation and heat shock protein responses in hypertensive rats. *J Cereb Blood Flow Metab.* 2005;25:878–886.
17. Nagai N, Noda K, Urano T, et al. Selective suppression of pathologic, but not physiologic, retinal neovascularization by blocking the angiotensin II type 1 receptor. *Invest Ophthalmol Vis Sci.* 2005;46:1078–1084.
18. Downie LE, Pianta MJ, Vingrys AJ, Wilkinson-Berka JL, Fletcher EL. AT1 receptor inhibition prevents astrocyte degeneration and restores vascular growth in oxygen-induced retinopathy. *Glia.* 2008;56:1076–1090.
19. Hirooka K, Baba T, Fujimura T, Shiraga F. Prevention of visual field defect progression with angiotensin-converting enzyme inhibitor in eyes with normal-tension glaucoma. *Am J Ophthalmol.* 2006;142:523–525.
20. Hasizume K, Mashima Y, Fumayama, et al. Genetic polymorphisms in the angiotensin II receptor gene and their association with open-angle glaucoma in a Japanese population. *Invest Ophthalmol Vis Sci.* 2005;46:1993–2001.
21. Sawada A, Neufeld AH. Confirmation of the rat model of chronic, moderately elevated intraocular pressure. *Exp Eye Res.* 1999;69:525–531.
22. Neufeld AH, Sawada A, Becker B. Inhibition of nitric-oxide synthase 2 by aminoguanidine provides neuroprotection of retinal ganglion cells in a rat model of chronic glaucoma. *Proc Natl Acad Sci USA.* 1999;96:9944–9948.
23. Lu Q, Zhu Y, Wong PT. Neuroprotective effects of candesartan against cerebral ischemia in spontaneously hypertensive rats. *Neuroreport.* 2005;16:1963–1967.
24. Costagliola C, Verolino M, de Rosa ML, Iaccarino G, Ciancaglini M, Mastropasqua L. Effect of oral losartan potassium administration on intraocular pressure in normotensive and glaucomatous human subjects. *Exp Eye Res.* 2000;71:167–171.
25. Laquis S, Chaudhary P, Sharma SC. The patterns of retinal ganglion cell death in hypertensive eyes. *Brain Res.* 1998;784:100–104.
26. Ausinsch B, Munson ES, Levy NS. Intraocular pressure in children with glaucoma during halothane anesthesia. *Am J Ophthalmol.* 1977;9:1391–1394.
27. Hetherington J, Shaffer RN. Tonometry and tonography in congenital glaucoma. *Invest Ophthalmol.* 1968;7:134–137.
28. Pease ME, Hammond JC, Quigley HA. Manometric calibration and comparison of TonoLab and TonoPen tonometers in rats with experimental glaucoma and in normal mice. *J Glaucoma.* 2006;15:512–519.
29. Ohashi M, Aihara M, Saeki T, Araie M. Efficacy of TonoLab in detecting physiological and pharmacological changes in rat intraocular pressure: comparison of TonoPen and microneedle manometry. *Jpn J Ophthalmol.* 2008;52:399–403.
30. Moore CC, Milne T, Morrison JC. Noninvasive measurement of rat intraocular pressure with the Tono-Pen. *Invest Ophthalmol Vis Sci.* 1993;34:363–369.
31. Saupe KW, Sobol SC, Koh SG, Apstein CS. Effect of AT1 receptor block begun late in life on normal cardiac aging in rats. *J Cardiovasc Phalmacol.* 2003;42:573–580.
32. Kurihara T, Ozawa Y, Shinoda K, et al. Neuroprotective effects of angiotensin II type 1 receptor (AT1R) blocker, telmisartan, via modulating AT1R and AT2R signaling in retinal inflammation. *Invest Ophthalmol Vis Sci.* 2006;47:5545–5552.
33. Griendling KK, Sorescu D, Ushio-Fukai M. NAD(P)H oxidase: role in cardiovascular biology and disease. *Circ Res.* 2000;86:494–501.
34. Zalba G, San Josè G, Moreno MU, et al. Oxidative stress in arterial hypertension: role of NAD(P)H oxidase. *Hypertension.* 2001;38:1395–1399.
35. Mattson MP. Apoptosis in neurodegenerative disorders. *Nat Rev Mol Cell Biol.* 2000;1:120–129.
36. Garcia-Valenzuela E, Shareef S, Walsh J, Sharma SC. Programmed cell death of retinal ganglion cells during experimental glaucoma. *Exp Eye Res.* 1995;61:33–44.
37. McKinnon SJ, Lehman DM, Kerrigan-Baumrind LA, et al. Caspase activation and amyloid precursor protein cleavage in rat ocular hypertension. *Invest Ophthalmol Vis Sci.* 2002;43:1077–1087.
38. Weinreb RN, Khaw PT. Primary open-angle glaucoma. *Lancet.* 2004;363:1711–1720.

Unintentional Displacement of the Retina after Standard Vitrectomy for Rhegmatogenous Retinal Detachment

Chieko Shiragami, MD, Fumio Shiraga, MD, Hidetaka Yamaji, MD, Kouki Fukuda, MD, Mai Takagishi, MD, Misako Morita, Co, Takehiro Kishikami, Co

Objective: To study unintentional displacement of the retina after standard vitrectomy for rhegmatogenous retinal detachment (RRD).

Design: Prospective interventional case series.

Participants: Forty-three eyes of 43 consecutive patients with cystic RRD involving 1 or more quadrants underwent successful standard vitrectomy with 20% sulfur hexafluoride gas injection. Neither scleral buckling nor retinotomy was performed.

Methods: Fundus autofluorescence (FAF) imaging was subsequently recorded to detect displacement of the retina using the Topcon TRC-50DX (Topcon, Tokyo, Japan) at 10 days and 1, 3, and 6 months postoperatively. Fluorescein angiography was also recorded using standard techniques for patients with abnormal FAF findings. Cyclotorsion and vertical deviation were measured postoperatively.

Main Outcome Measures: The proportion of eyes with postoperative retinal displacement detected by FAF imaging.

Results: The mean age of these 43 patients was 60 years with a range of 39 to 77 years. Of the 43 eyes, retinal detachment involved 1 quadrant in 2 eyes, 2 quadrants in 31 eyes, 3 quadrants in 8 eyes, and 4 quadrants in 2 eyes. After complete reattachment of the retina, FAF photography demonstrated hyperfluorescent lines superiorly parallel to retinal vessels within the vascular arcade in 27 of the 43 eyes (62.8%). Fluorescein angiography did not demonstrate any abnormalities corresponding to the linear autofluorescence. This autofluorescence was hypothesized to originate from increased metabolic activity of the retinal pigment epithelium that had been preoperatively located under the major retinal vessels and was postoperatively exposed to light because of downward displacement of the retina. Of the 27 eyes with retinal displacement, 1 to 5 degrees of extorsion were seen in 16 eyes (59.3%), and 1 to 4 degrees of vertical deviation were seen in 13 eyes (48.1%). None of the 27 patients had diplopia or slant. The extent of retinal detachment ($P = 0.019$) and the macular status (on or off) ($P = 0.016$) were significantly associated with postoperative displacement of the retina.

Conclusions: In eyes with RRD treated with standard vitrectomy and gas injection, the retina may move downward after the surgery. If the extent of retinal detachment is large, or macular detachment is present, unintentional postoperative retinal translocation may easily occur.

Financial Disclosure(s): The author(s) have no proprietary or commercial interest in any materials discussed in this article. *Ophthalmology 2009;xx:xxx © 2009 by the American Academy of Ophthalmology.*

The commonly used treatments for rhegmatogenous retinal detachment (RRD) are scleral buckling surgery and primary pars plana vitrectomy (PPV).[1,2] Pneumatic retinopexy or scleral buckling is usually performed for localized cases. At the other end of the spectrum, complicated cases with proliferative vitreoretinopathy, giant tears, bullous RRD, and retinal breaks with marked vitreous traction are commonly treated with primary PPV. Pars plana vitrectomy surgery for retinal detachments has become safer and more effective using perfluorocarbon liquids (PFCL).[3]

Inferior limited macular translocation with scleral imbrication was performed to move the posterior retina downward and translocate the fovea outside a choroidal neovascular membrane.[4–6] However, as de Juan and Vander reported in 1999,[7] creation of retinal detachment and air tamponade without scleral imbrication could move the retina downward. Even if the retina is totally reattached during PPV, in patients with RRD, subtle subretinal fluid remains at the end of surgery. After the surgery, the patients usually take a sitting position for a while before they maintain an appropriate position. At that time, force of gravity may slightly move the retina downward. Thus, we aimed to study unintentional displacement of the retina after standard vitrectomy for RRD by using fundus autofluorescence (FAF).

Materials and Methods

Patients

Forty-three eyes of 43 consecutive patients with RRD involving 1 or more quadrants underwent successful standard PPV with 20%

ISSN 0161-6420/09/$–see front matter
doi:10.1016/j.ophtha.2009.06.025

sulfur hexafluoride gas injection at the Kagawa University Hospital between November 2006 and June 2008. The mean age of all patients (26 male, 17 female) was 60.0 years with a range of 39 to 77 years. No patients had binocular diplopia in their preoperative history. The eyes with reoperations, silicon oil tamponade, or proliferative vitreoretinopathy were excluded from this study. The study was conducted in accordance with the recommendations of the Declaration of Helsinki and was approved by the institutional review board at the Kagawa University Hospital. After an explanation of the purpose of the study and the procedures to be used, a signed informed consent was obtained from all patients before surgery and examinations.

Surgical Technique

Local anesthesia was induced by retrobulbar nerve block. A 3-port PPV was performed in all cases using the Accurus vitrectomy system (Alcon Labs, Fort Worth, TX). The patients aged more than 50 years underwent combined cataract surgery. The posterior hyaloid was separated and removed using the vitreous cutter. After that, all vitreous traction on retinal tears was removed and the peripheral vitreous was subtotally shaved. In 30 eyes, PFCL was injected over the posterior pole and reached the posterior border of retinal breaks through a 20- or 23-gauge blunt cannula. Fluid–air exchange was performed to drain the subretinal fluid through original retinal breaks in all 43 eyes. After endolaser photocoagulation around retinal breaks was performed and PFCL was completely removed, 20% sulfur hexafluoride gas was used for internal tamponade in all cases. Neither scleral buckling nor retinotomy was performed. The patients did not take a face-down positioning but performed a sitting position for several minutes before they went back to the recovery room after the operation. After that, face-down or appropriate positioning was maintained for 7 to 10 days after the surgery.

Ophthalmic Examinations and Fundus Photography

All patients underwent a regular ophthalmic examination, including measurement of the best-corrected visual acuity and fundus examination. Color fundus photography and fluorescein angiography using the Topcon TRC-50DX fundus camera (Topcon, Tokyo, Japan) were carried out preoperatively and postoperatively in all eyes.

Color fundus photography was performed using 50-degree fields of the panoramic image preoperatively and postoperatively (10 days and 1, 3, and 6 months after PPV in all patients, and 12 months after PPV in 4 patients). The FAF imaging was recorded to detect displacement of the retina using the Topcon TRC-50DX fundus camera with 2 bandpass filters (based on the modification by Spaide with an excitation bandwidth of 500–610 nm and an emission bandwidth of 675–715 nm)[8] at 10 days, 1 month, 3 months, and 6 months after the surgery. Fluorescein angiography was also recorded using standard techniques for patients with abnormal FAF findings.

Orthoptic Examination

All patients underwent an orthoptic examination 3 months after surgery. A synoptophore (Clement and Clark, Edinburgh, UK) was used to measure the objective and subjective angles of deviation and fusion ability.[9] The elevation-dependent torsional disparity during various degrees of convergence was measured. With a synoptophore, the subject views 2 images at optical infinity through 2 eyepieces. These images fill the visual field so that nothing in the surrounding laboratory is seen. The images can be rotated vertically and torsionally about a Fick system of gimbals, independently for each eye.

Statistical Methods

To determine whether there was a significant association among several factors (independent variables), including age, gender, PFCL use, macular status (on or off) and extent of retinal detachment, and unintentional displacement of the retina (dependent variable), multiple logistic regression analysis was performed. A P value of less than 0.05 was considered significant. This statistical analysis was carried out using SPSS 11.5 statistical software (SPSS Inc., Chicago, IL).

Results

On preoperative fundus examinations, 43 eyes had bullous RRD involving 1 or more quadrants. Of the 43 eyes, RRD involved 1

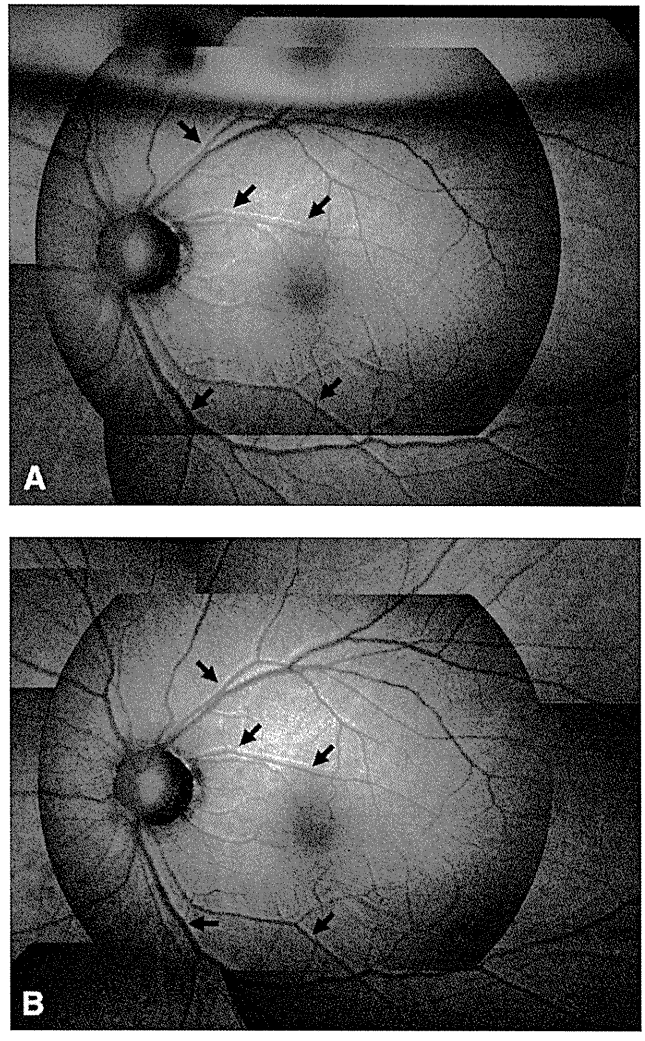

Figure 1. A, The fundus autofluorescence (FAF) image taken 10 days postoperatively demonstrates hyperfluorescent lines (*arrows*) parallel to retinal vessels. **B,** The FAF image taken 3 months postoperatively demonstrates that the hyperfluorescent lines are morphologically identical to those observed 10 days postoperatively in their form, range, and brightness (*arrows*).

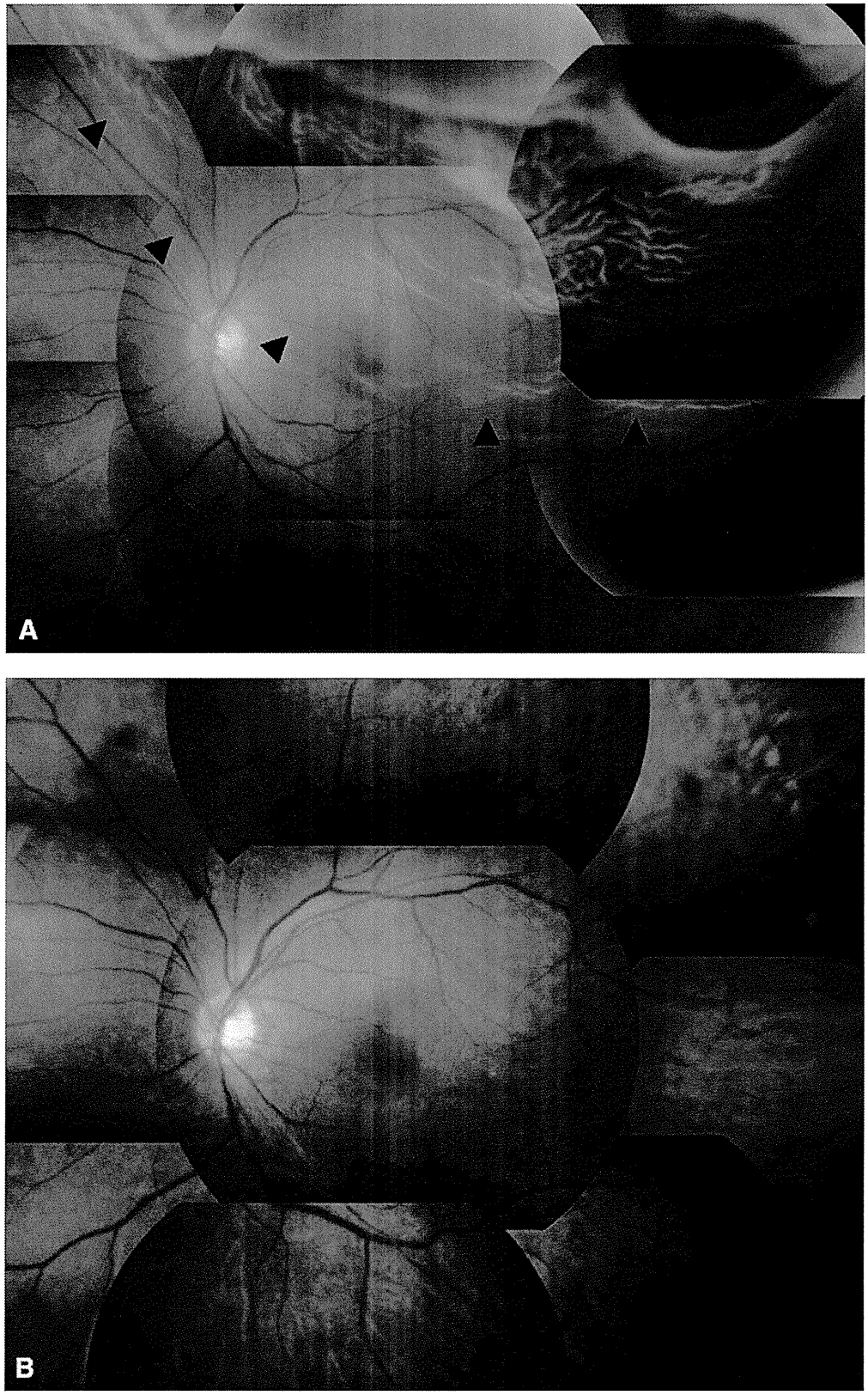

Figure 2. A, Preoperative color photograph of the eye with cystic rhegmatogenous retinal detachment (RRD). The retinal tear is present in the temposuperior region. The RRD demarcation line (*arrowheads*). **B,** Color photograph taken 1 month postoperatively. The retina is attached completely. **C,** The fundus autofluorescence (FAF) image taken 1 month postoperatively demonstrates hyperfluorescent lines also in the region where there was no retinal detachment before surgery (*arrowheads*).

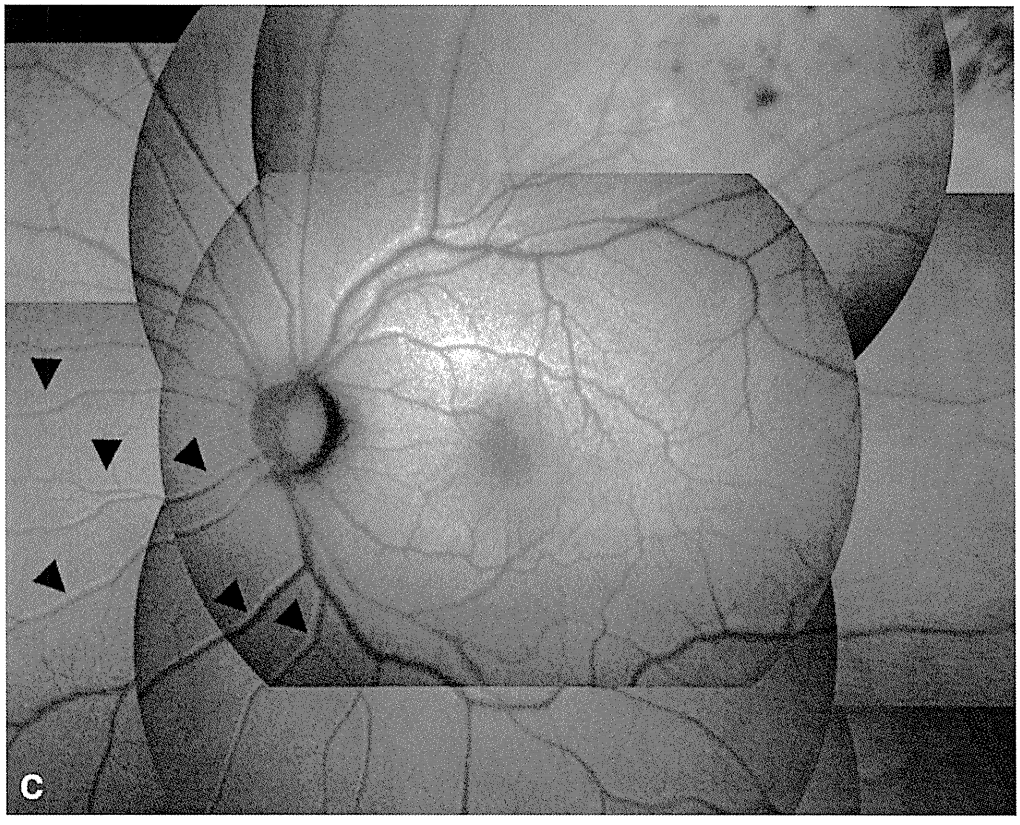

Figure 2. (Continued.)

quadrant in 2 eyes, 2 quadrants in 31 eyes, 3 quadrants in 8 eyes, and 4 quadrants in 2 eyes on fundus examination. Retinal breaks were located in the superior region (19 eyes), the temporal region (13 eyes), the nasal region (5 eyes), the inferior region (1 eye), and multiple regions (5 eyes).

After complete reattachment of the retina, autofluorescence photography demonstrated hyperfluorescent lines superiorly parallel to the retinal vessels in 27 of the 43 eyes (62.8%). This autofluorescence was hypothesized to originate from increased metabolic activity of the retinal pigment epithelium (RPE) that had been preoperatively located under the major retinal vessels and was postoperatively exposed to light because of downward displacement of the retina. The clinical findings of 27 patients whose retina moved downward postoperatively are shown in Table 1 (available at http://aaojournal.org). These hyperfluorescent lines on FAF images were observed 10 days after PPV (Fig 1A), and these lines were morphologically identical to those taken 3 months postoperatively in their form, range, and brightness (Fig 1B). In 3 of 27 eyes, hyperfluorescent lines parallel to retinal vessels were also observed in the region where there had been no retinal detachment before surgery (Fig 2). However, in 4 eyes of 4 patients who were followed over 12 months, the hyperfluorescent lines moved slightly closer to the original retinal vessels (Fig 3). In the 27 eyes, fluorescein angiography did not demonstrate any abnormalities corresponding to the linear autofluorescence (Fig 4). On the other hand, there were no significant FAF abnormalities in the remaining 16 eyes (37.2%).

Multiple logistic regression analysis revealed that the extent of retinal detachment ($P = 0.019$) and the macular status (on or off) ($P = 0.016$) were significantly associated with postoperative retinal displacement (Table 2).

In the 27 patients whose eyes showed unintentional displacement of the retina with macular rotation around the disc, postoperative examination with a synoptophore revealed 1 to 5 degrees of extorsion in 16 patients (59.3%) and 1 to 4 degrees of vertical deviation in 13 patients (48.1%) (Table 1, available at http://aaojournal.org). However, none of the 27 patients had cyclovertical diplopia or slant. The remaining 16 patients with no displacement of the retina did not have obvious strabismic deviation by examination with a synoptophore.

Discussion

Fundus autofluorescence is a noninvasive test that provides discrete funduscopic images based on stimulated emission of light from lipofuscin. Lipofuscin is a cellular waste product containing lipid, protein, and fluorophores such as A2E. Visualization of the signal depends on the distribution pattern of the fluorophore-containing lipofuscin.[10–12] FAF imaging allows topographic mapping of lipofuscin distribution in the RPE cell monolayer, as well as of other fluorophores that may occur with disease in the outer

Figure 3. **A,** The fundus autofluorescence (FAF) image taken 10 days postoperatively demonstrates the hyperfluorescent lines. **B,** The FAF image taken 12 months postoperatively demonstrates the hyperfluorescent lines. These hyperfluorescent lines appear to be closer to the original retinal vessels than those observed 10 days postoperatively.

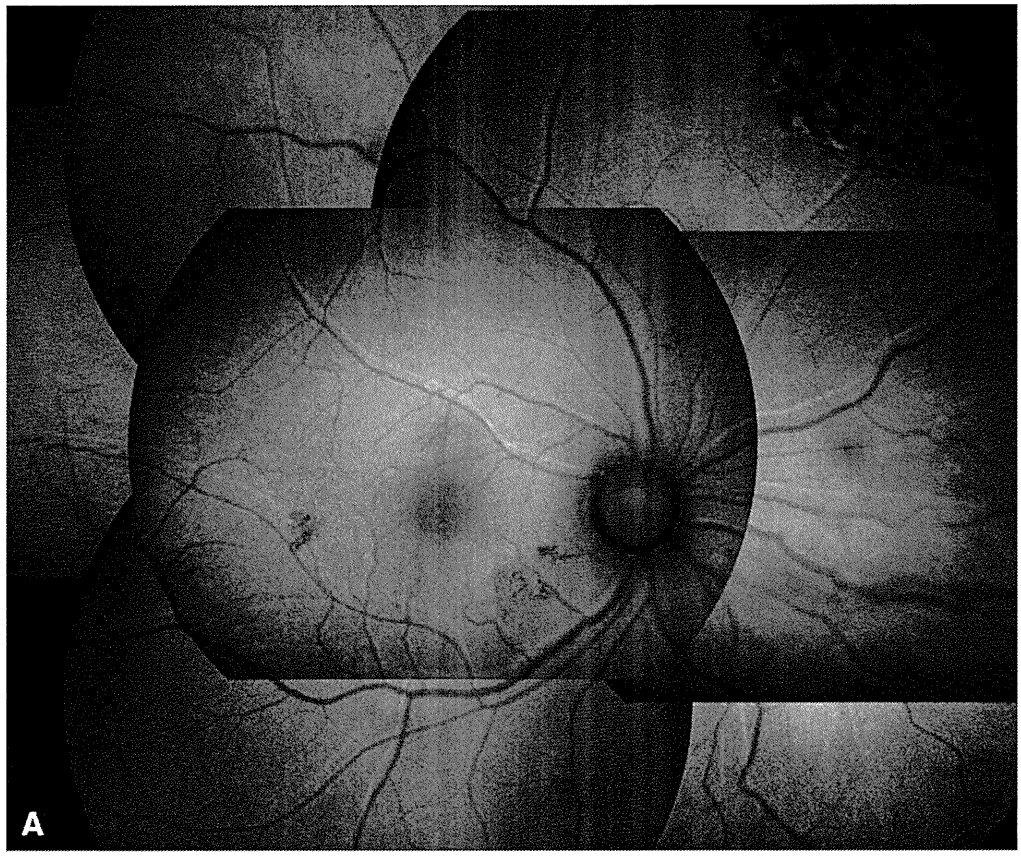

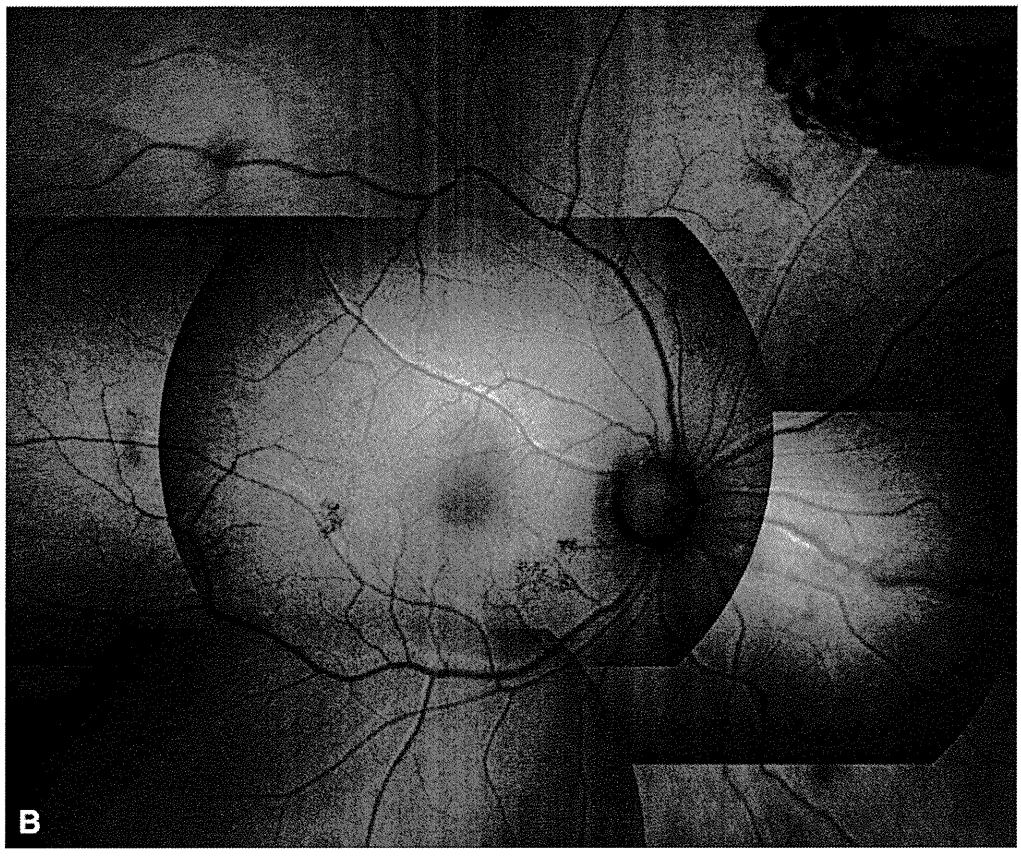

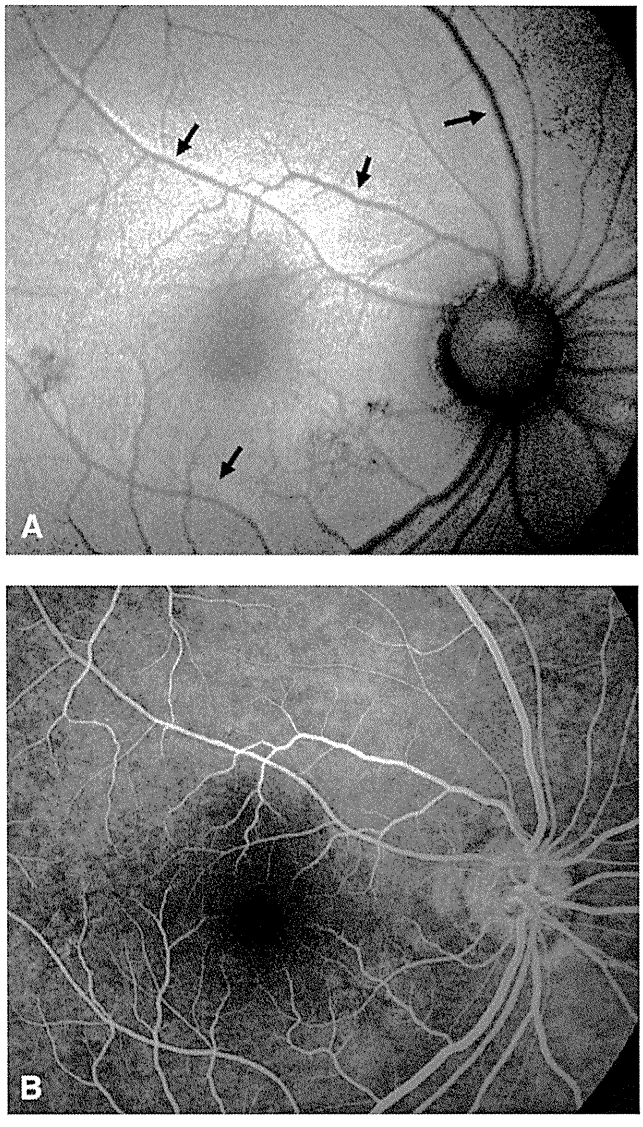

Figure 4. A, The fundus autofluorescence (FAF) image taken 3 months postoperatively (the same eye as Figure 3). Hyperfluorescent lines (*arrows*). B, The fluorescein angiography does not demonstrate any abnormalities corresponding to the linear autofluorescence.

retina and the subneurosensory space.[8] Fundus autofluorescence in the RPE is dependent on outer segment renewal and potentially affected by a balance between accumulation and clearance. Therefore, the autofluorescence can be interpreted as a clinical sign for the metabolic activity of the RPE. Increased phagocytosis of photoreceptor outer segments gives rise to hyperautofluorescence.[8,12] FAF imaging, therefore, is a valuable technique for the assessment of unintentional displacement of the retina after standard vitrectomy for patients with RRD. The reason why increased autofluorescence indicates the preoperative site of retinal vessels is unclear. For a long time, the RPE cells beneath the retinal vessels were prevented from light irradiation, in other words, they maintained dark adaptation because they were shaded by the retinal vessels. After that, acute exposure to the excitation light, which was caused by translocation of the retinal vessels, may have induced increased FAF signals.[12] Because fluorescein angiography did not demonstrate any abnormalities corresponding to the linear autofluorescence, it is considered that these hyperautofluorescent lines might be due to metabolic changes in RPE cells, but not morphologic changes. The hyperfluorescent lines on FAF images observed 10 days after PPV were morphologically identical to those taken 3 months postoperatively in their form, range, and brightness. However, in 4 eyes of 4 patients who were followed over 12 months, the hyperfluorescent lines moved slightly closer to the original retinal vessels. The retina might return to the preoperative, original position with times.

Immediately after the end of PPV surgery, a little subretinal fluid usually remains, despite intraocular gas tamponade. The fact that the retina moved downward suggests that intraocular gas could move the retina downward because of the shift of residual subretinal fluid during the sitting position immediately after PPV surgery. Large retinal detachment including macular detachment, which was independently associated with postoperative displacement of the retina, may easily shift residual subretinal fluid downward. The patients did not take a face-down position but took a sitting position for several minutes before they went back to the recovery room after the operation. If patients take the strict prone position as soon as the operation is completed, retinal displacement may be prevented.

If the macula is translocated vertically around the disk but not the fovea, cyclotorsional diplopia or awareness of a tilted image is likely to occur.[13,14] However, the cyclodeviation could be easily compensated for by the sensory fusion ability, which is driven by the central nervous system, without a clinically visible motor adaptation.[15] Limited macular translocation or full macular translocation with 360-degree retinotomy surgery has been performed for age-related macular degeneration.[4–6,16-18] The retina in the macula is relocated to a new location away from the subretinal pathology, overlying healthier RPE. In the majority of cases undergoing full macular translocation, the macula is rotated upward, creating intorsion in the operated eye. The rotation of the retina leads to horizontal and vertical strabismus. This torsion also greatly exceeds the maximum total amplitude of cyclofusion, which can be as large as 15 degrees.[11,19,20] Extraocular muscle surgery can reduce cyclotorsion after macular translocation surgery, alleviating symptoms of tilted vision and

Table 2. Multiple Logistic Regression Model of Variables Associated with Displacement of Retina

		Standard	
	OR	*95% CI*	*P Value*
Age	1.064	0.971–1.167	0.184
Gender	3.022	0.595–15.347	0.182
Quadrants of RD	7.743	1.409–42.569	0.019
Macula status (0, on; 1, off)	10.909	1.560–76.290	0.016
PFCL use (0, not use; 1, use)	0.697	0.135–3.599	0.667

CI = confidence interval; OR = odds ratio; PFCL = perfluorocarbon liquids; RD = retinal detachment.

facilitating use of the vision in the translocated eye.[13,14] In the present study, 1 to 5 degrees of extorsion were seen in 16 of the 27 eyes (59.3%) and 1 to 4 degrees of vertical deviation were seen in 13 of 27 eyes (48.1%) that had unintentional displacement of the retina after PPV for RRD. Because normal subjects have no vertical deviation and little cyclodeviation, cyclotorsion and vertical deviation were thought to be caused by the displacement of the retina.[21,22] Cyclotorsion and vertical deviation can be compensated for by the sensory and motor fusion ability. In fact, none of the 27 patients had binocular diplopia or slant. However, there is a possibility that larger-angle extorsion or vertical deviation may occur after PPV in patients with RRD, resulting in unexpected binocular diplopia. Therefore, patients with RRD must be followed carefully after PPV, especially with respect to their binocular vision, except for the patients with poor vision at the affected eyes.

In conclusion, the current study suggests that the retina may move downward postoperatively in eyes with cystic RRD treated with standard vitrectomy and gas injection. If there is large retinal detachment, or macular detachment is present, unintentional postoperative retinal translocation may easily occur. Despite the fact that approximately half of the patients demonstrated excyclotorsion or vertical deviation on orthoptic examination, no patients had binocular diplopia. A long-term FAF study after PPV for RRD may help to identify the position shift trend of the retina, and the disappearance of the line may help to better understand the RPE metabolism.

References

1. Heimann H, Bartz-Shmidt KU, Bornfeld N, et al. Scleral Buckling versus Primary Vitrectomy in Rhegmatogenous Retinal Detachment Study. Scleral buckling versus primary vitrectomy in rhegmatogenous retinal detachment: a prospective randomized multicenter clinical study. Ophthalmology 2007; 114:2142–54.
2. Stangos AN, Petropoulos IK, Brozou CG, et al. Pars-plana vitrectomy alone vs vitrectomy with scleral buckling for primary rhegmatogenous pseudophakic retinal detachment. Am J Ophthalmol 2004;138:952–8.
3. Comaratta MR, Chang S. Perfluorocarbon liquids in the management of complicated retinal detachments. Curr Opin Ophthalmol 1991;2:291–8.
4. de Juan E Jr, Loewenstein A, Bressler NM, Alexander J. Translocation of the retina for management of subfoveal choroidal neovascularization II: a preliminary report in humans. Am J Ophthalmol 1998;125:635–46.
5. Pieramici DJ, de Juan E Jr, Fujii GY, et al. Limited inferior macular translocation for the treatment of subfoveal choroidal neovascularization secondary to age-related macular degeneration. Am J Ophthalmol 2000;130:419–28.
6. Morizane Y, Shiraga F, Takasu I, et al. Selection for inferior limited macular translocation on the basis of distance from the fovea to the inferior edge of the subfoveal choroidal neovascularization. Am J Ophthalmol 2002;133:848–50.
7. de Juan E Jr, Vander JF. Effective macular translocation without scleral imbrication. Am J Ophthalmol 1999;128:380–2.
8. Spaide RF. Autofluorescence from the outer retina and subretinal space: hypothesis and review. Retina 2008;28:5–35.
9. Sen DK, Singh B, Mathur GP. Torsional fusional vergences and assessment of cyclodeviation by synoptophore method. Br J Ophthalmol 1980;64:354–7.
10. Spaide RF. Fundus autofluorescence and age-related macular degeneration. Ophthalmology 2003;110:392–9.
11. Chung JE, Spaide RF. Fundus autofluorescence and vitelliform macular dystrophy. Arch Ophthalmol 2004;122:1078–9.
12. Schmitz-Valckenberg S, Holz FG, Bird AC, Spaide RF. Fundus autofluorescence imaging: review and perspectives. Retina 2008;28:385–409.
13. Holgado S, Enyedi LB, Toth CA, Freedman SF. Extraocular muscle surgery for extorsion after macular translocation surgery: new surgical technique and clinical management. Ophthalmology 2006;113:63–9.
14. Ohtsuki H, Shiraga F, Morizane Y, et al. Transposition of the anterior superior oblique insertion as a treatment for excyclotorsion induced from limited macular translocation. Am J Ophthalmol 2004;137:125–34.
15. Guyton DL. Ocular torsion: sensorimotor principles. Graefes Arch Clin Exp Ophthalmol 1988;226:241–5.
16. Machemer R, Steinhorst UH. Retinal separation, retinotomy, and macular relocation: II. A surgical approach for age-related macular degeneration? Graefes Arch Clin Exp Ophthalmol 1993;231:635–41.
17. Eckardt C, Eckardt U, Conrad HG. Macular rotation with and without counter-rotation of the globe in patients with age-related macular degeneration. Graefes Arch Clin Exp Ophthalmol 1999;237:313–25.
18. Ohji M, Fujikado T, Kusaka S, et al. Comparison of three techniques of foveal translocation in patients with subfoveal choroidal neovascularization resulting from age-related macular degeneration. Am J Ophthalmol 2001;132:888–96.
19. Guyton DL. Clinical assessment of ocular torsion. Am Orthopt J 1983;33:7–15.
20. von Noorden GK. Clinical and theoretical aspects of cyclotropia. J Pediatr Ophthalmol Strabismus 1984;21:126–32.
21. Rutstein RT, Corliss DA. The relationship between duration of superior oblique palsy and vertical fusional vergence, cyclodeviation, and diplopia. J Am Optom Assoc 1995;66:442–8.
22. Nomura H, Yamgasaki T, Awaya S. Effect of tilting on cyclodeviation in nine diagnostic positions of gaze in normal subjects with Awaya's new cyclo test [in Japanese]. Nippon Ganka Gakkai Zasshi 1995;99:1030–5.

Footnotes and Financial Disclosures

Originally received: February 11, 2009.
Final revision: May 22, 2009.
Accepted: June 11, 2009.
Available online: ●●●. Manuscript no. 2009-186.

Department of Ophthalmology, Kagawa University Faculty of Medicine, Kagawa, Japan.

Financial Disclosure(s):
The author(s) have no proprietary or commercial interest in any materials discussed in this article.

Correspondence:
Chieko Shiragami, MD, Department of Ophthalmology, Kagawa University School of Medicine, 1750-1 Ikenobe Miki-cho, Kagawa 761-0793, Japan. E-mail: chappi@kms.ac.jp.

Table 1. Clinical Characteristics of 27 Patients Whose Retina Moved Downward Postoperatively

Case No.	Gender	Affected Eye	Age (yrs)	Preoperative VA	Postoperative VA	Quadrants of RD	Macula Status	PFCL Use	Postoperative Cyclodeviation	Postoperative Vertical Deviation
1	M	L	76	0.2	1	3	off	+	Ex3°	L/R2°
2	M	L	47	0.5	0.9	3	off	+	Ex5°	L/R1°
3	M	R	53	0.4	0.9	2	off	+	0°	0°
4	M	R	59	0.3	0.6	2	off	+	Ex1°	R/L2°
5	F	R	58	0.01	0.5	4	off	+	Ex3°	R/L2°
6	M	L	61	1.2	1.2	2	on	−	0°	0°
7	F	L	64	1.2	0.7	2	on	+	0°	0°
8	F	R	58	0.04	0.5	3	off	−	0°	0°
9	M	L	65	0.9	1.2	2	on	+	0°	0°
10	M	R	63	0.8	1	2	off	+	0°	R/L4°
11	F	L	65	0.1	0.6	2	off	+	0°	0°
12	F	R	56	1.2	1.5	2	on	+	Ex3°	R/L2°
13	F	L	75	0.5	0.8	3	on	−	Ex3°	L/R2°
14	F	L	64	0.09	1.2	3	off	+	0°	0°
15	F	L	60	0.9	1.2	1	on	+	0°	0°
16	M	L	72	0.03	0.4	2	off	−	Ex5°	L/R4°
17	M	R	77	L.S.	0.4	3	off	−	Ex3°	R/L2°
18	F	L	67	0.04	0.4	4	off	+	Ex5°	L/R3°
19	F	R	56	1.2	1.5	2	on	−	Ex3°	R/L2°
20	M	R	39	1	0.5	2	on	−	0°	0°
21	M	L	53	1.2	1.2	2	on	+	0°	0°
22	M	L	61	1.5	1.5	2	on	+	Ex2°	0°
23	M	R	58	0.04	1.2	2	off	+	Ex3°	R/L2°
24	M	R	58	0.01	0.5	3	off	+	Ex3°	0°
25	M	L	64	0.7	1	2	on	+	Ex5°	L/R1°
26	M	L	57	0.04	0.7	3	off	+	Ex5°	0°
27	M	L	67	2	1	1	on	−	Ex2°	0°

Ex = extorsion; L = left; PFCL = perfluorocarbon liquids; R = right; RD = retinal detachment; VA = visual acuity.

Neuroscience Letters 462 (2009) 267–271

Contents lists available at ScienceDirect

Neuroscience Letters

journal homepage: www.elsevier.com/locate/neulet

A novel missense mutation (Leu46Val) of *PAX6* found in an autistic patient

Motoko Maekawa[a,*], Yoshimi Iwayama[a], Kazuhiko Nakamura[b], Miho Sato[c], Tomoko Toyota[a], Tetsuo Ohnishi[a], Kazuo Yamada[a], Taishi Miyachi[d], Masatsugu Tsujii[d,e], Eiji Hattori[a], Nobuo Maekawa[f], Noriko Osumi[g,h], Norio Mori[b], Takeo Yoshikawa[a,h]

[a] *Laboratory for Molecular Psychiatry, RIKEN Brain Science Institute, 2-1 Hirosawa, Wako, Saitama 351-0198, Japan*
[b] *Department of Psychiatry and Neurology, Hamamatsu University School of Medicine, Shizuoka, Japan*
[c] *Department of Ophthalmology, Hamamatsu University School of Medicine, Shizuoka, Japan*
[d] *The Osaka-Hamamatsu Joint Research Center for Child Mental Development, Hamamatsu University School of Medicine, Shizuoka, Japan*
[e] *Faculty of Sociology, Chukyo University, Toyota, Japan*
[f] *Maekawa Eye Clinic, Miyagi, Japan*
[g] *Department of Developmental Neurobiology, Tohoku University Graduate School of Medicine, Miyagi, Japan*
[h] *CREST, Japanese Science and Technology Agency, Tokyo, Japan*

ARTICLE INFO

Article history:
Received 28 May 2009
Received in revised form 3 July 2009
Accepted 6 July 2009

Keywords:
PAX6
Missense mutation
Autism
Aniridia

ABSTRACT

The paired box 6 (PAX6) is a transcription factor expressed early in development, predominantly in the eye, brain and pancreas. Mutations in *PAX6* are responsible for eye abnormalities including aniridia, and it is also known that some *PAX6* mutations result in autism with incomplete penetrance. We resequenced all the exons and flanking introns of *PAX6* in 285 autistic patients in the Japanese, with the possibility that novel mutations may underlie autism. Fifteen different polymorphisms were identified: 13 are novel, and 2 were previously reported (rs667773 and rs3026393). Among the novel ones, there is one missense mutation that was found in a patient: 136C > G (Leu46Val) (single nucleotide polymorphism ID "ss130452457" is temporarily assigned). Leu46 is extremely conserved from fly to human, and we did not detect Val46 in 2120 nonautistic subjects. The autistic patient carrying this heterozygous mutation showed reduced vision, photophobia and eyelid ptosis, but no other ocular abnormality such as aniridia. Our findings suggest the necessity of further studies on the causal relationship between *PAX6* and autism.

The human paired box 6 (*PAX6*) gene is located on chromosome 11p13, and its orthologues have been found in diverse species. This gene encodes a transcription factor that is involved in multiple developmental pathways and is expressed early in the development of the eye, numerous regions of the brain, and the pancreas [25]. The *PAX6* gene of 22 kb size contains 14 exons, including an alternatively spliced exon 5a that encodes 14 amino acids, and encodes a protein of 422 amino acid (Fig. 1). The PAX6 protein contains two DNA-binding domains (one paired domain and one homeodomain), and one proline/serine/threonine-rich (PST) transactivation domain. PAX6 affects the development of the nervous system and brain by regulating proneural genes such as neurogenin 2 (*Ngn2*) and achaete–scute complex homolog-like 1 (*Mash-1*) [28,36]. The *Pax6* heterozygous mutant mice and rats, i.e., "*small eye*", show both ocular and neuronal phenotypes including an absent olfactory bulb, a decrease in the number of cortical neurons and cortical plate thickness, as well as altered dorsoventral patterning of the forebrain, and a decrease in hippocampal neurogenesis at the postnatal stage [18].

In human, in addition to the reports of associations of various *PAX6* mutations with eye abnormalities including syndromic ones like Peters anomaly [8,26], there is emerging evidence of the roles of *PAX6* mutations in behavioral and neurodevelopmental disease phenotypes such as autism and mental retardation. For instance, recent studies have identified individuals with *PAX6* mutations who manifest mental retardation and aniridia [12,20,32]. In addition, magnetic resonance imaging (MRI) studies of patients with aniridia have shown subtle brain abnormalities including a lack of the anterior commisure and pineal gland [23]. These accumulating lines of evidence suggest that concomitant phenotypes are determined by the nature of *PAX6* mutations. In this study, we carried out resequencing analysis of the gene in autistic patients with, with the aim of searching for additional mutations of *PAX6*, which might be associated with the disease.

Two hundred and eighty-five autistic patients of Japanese descent (236 men, 49 women; age, from 3 to 32 years old) were analyzed. The diagnosis of autism was made on the basis of the Autism Diagnostic Interview-Revised (ADI-R) criteria [17] with consensus from at least two experienced psychiatrists. All available medical

* Corresponding author. Tel.: +81 48 467 5968; fax: +81 48 467 7462.
E-mail address: mmaekawa@brain.riken.jp (M. Maekawa).

0304-3940/$ – see front matter © 2009 Elsevier Ireland Ltd. All rights reserved.
doi:10.1016/j.neulet.2009.07.021

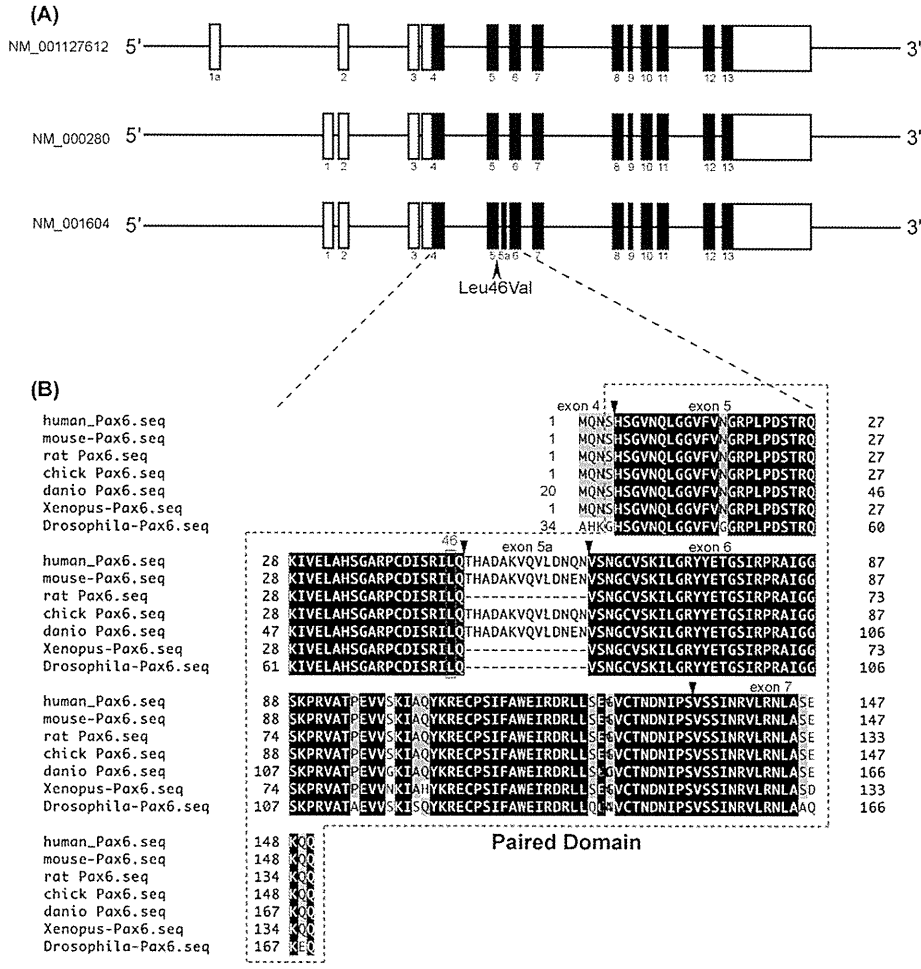

Fig. 1. Genomic structure of human *PAX6* and amino acid sequences of PAX6/Pax6. (A) Genomic structure and location of 136G (Val46) missense mutation for human *PAX6*. Exons are denoted by boxes, with untranslated regions in white and translated regions in black. A black arrowhead indicates the location of the missense mutation. Note that the three isoforms are shown (http://genome.ucsc.edu/cgi-bin/hgGateway?org=human). (B) Amino acid sequence alignments of PAX6/Pax6 among species. The black boxes indicate the conserved amino acids from Drosophila to human. The grey boxes show the partially conserved ones. The conserved 46Leu is indicated by a red square. The red-broken-line box shows the paired domain that contains the conventional 128 residues [34] and five subsequent residues (SEKQQ) [38]. (For interpretation of the references to color in this figure caption, the reader is referred to the web version of the article.)

records were also taken into consideration. Regarding a detected missense mutation in patient samples, we analyzed 2120 nonautistic subjects, who are 1060 patients with schizophrenia (503 men, 557 women; mean age 48.0 ± 13.8 years) and 1060 controls who are free of mental disorders (503 men, 557 women; mean age 47.7 ± 13.6 years) [16]. All the subjects were from central Japan. The study was approved by the ethics committees of RIKEN and Hamamatsu University and was conducted in accordance with the Declaration of Helsinki (http://www.wma.net). All the participants provided written informed consent (for patients under 16 years old, we explained the aim of this study to the patients' parents and as long as possible to the patients in easy terms, and obtained written informed consent from at least their parents).

Genomic DNA was isolated from blood samples by standard methods. All the exons and exon/intron boundaries of *PAX6* were screened for polymorphisms by direct sequencing of polymerase chain reaction (PCR) products. The primers used for amplification are listed in Supplementary Table 1. PCR was performed with an initial denaturation at 95 °C for 10 min, followed by 35 cycles at 95 °C for 15 s, 60–63 °C (optimized for each primer pair) for 15 s, 72 °C for 30 s, and a final extension at 72 °C for 10 min, with AmpliTaqGold (Applied Biosystems, Foster City, CA) or it was performed with an initial denaturation at 98 °C for 5 min, followed by 35 cycles at 98 °C for 45 s, 58–61 °C for 30 s, 68 °C for 30 s, and a final extension at 68 °C for 10 min, with Pwo SuperYield DNA Polymerase (Roche, Basel, Switzerland). Direct sequencing of PCR products was performed with the BigDye Terminator v3.1 Cycle Sequencing kit (Applied Biosystems) and the ABI PRISM 3730*xl* Genetic Analyzer (Applied Biosystems). Polymorphisms were detected with the SEQUENCHER program (Gene Codes Corporation, Ann Arbor, MI). The genomic structure of *PAX6* is based on the UCSC March 2006 draft assembly of the human genome database (http://www.genome.ucsc.edu), and the NCBI (http://www.ncbi.nlm.nih.gov/) database was searched for known single nucleotide polymorphisms (SNPs). Custom TaqMan SNP Genotyping assays (Applied Biosystems) were used to score the identified missense SNP by the TaqMan assay method [27], and using ABI PRISM 7900 Sequence Detection System (SDS) and SDS v2.3 software (Applied Biosystems).

Our polymorphism screening detected a total of 15 different variants in the *PAX6*: 13 are novel (−11,521C > T, IVS4-85T > C, IVS4-70 ~ −72Ins/DelTCT, IVS4-42C > T, 117G > A, 136C > G, IVS5-163C > T, 319C > T, IVS6 + 28C > T, IVS8 + 14Ins/DelT, 867T > C, IVS12 + 11G > A and 1194C > T), and 2 were previously reported (rs667773 and rs3026393) (Table 1). With respect to novel variants, the 136C > G was a missense mutation (Leu46Val; ss130452457) located in the paired domain, which was found in one patient as a heterozygote (Table 1 and Fig. 1). We then examined 2120 nonautistic subjects for this missense mutation. However, the mutation was not detected

Table 1
PAX6 polymorphisms detected in 285 autistic patients in the Japanese.

Polymorphism[a]	dbSNP ID	Allele frequency
ATG ~ −11,521C > T	Novel	1/570
IVS4-85T > C	Novel	1/570
IVS4-70~72Ins/DelTCT	Novel	1/570
IVS4-42C > T	Novel	1/570
117G > A [Pro(CCG)39Pro(CCA)]	Novel	1/570
136C > G [Leu(CTG)46Val(GTG)]	Novel	1/570
IVS5-163C > T	Novel	1/570
319C > T [Leu(CTG)107LeuTTG]	Novel	1/570
IVS6 + 28C > T	Novel	1/570
IVS8 + 14Ins/DelT	Novel	1/570
IVS9-12C > T	rs667773	68/570
867T > C [Ser(AGT)289Ser(AGC)]	Novel	4/570
IVS12 + 11(G > A)	Novel	1/570
IVS12 + 43T > G	rs3026393	261/570
1194C > T [Ser(TCC)398Ser(TCT)]	Novel	4/570

[a] Major allele > minor allele; intron Nos. are based on the NM_000280 (Fig. 1A).

in these subjects. We also examined 252 Autism Genetic Resource Exchange (AGRE) trios (756 samples; http://www.agre.org), but again did not detect it.

The autistic patient with the *PAX6* missense mutation (Leu46Val) is a daughter of nonconsanguineous parents (Fig. 2), and the mutation was transmitted from her father. However, her father does not have autism, major depression, anxiety and social awkwardness implying a sign of autism upon psychiatric interview, as well as her mother and older brother. The patient's pregnancy and birth history were without any problems. At 1.5 years of age, she was assessed as developing normally except for mild speech delay. During her preschool days, she used to spend many hours playing alone. She attended a normal elementary school and a normal junior high school. However, she attended a high school for handicapped children because of her difficulty in learning at a normal high school. When she was 10 years old, she was diagnosed as having autism by an expert in childhood psychiatry. She had deficits in all three areas of communication, reciprocal social interaction and behavior. Her ADI-R scores were 17 in the social domain (cutoff = 10), 15 in the language (verbal) domain (cutoff = 8), and 6 in the repetitive/restrictive behaviors domain (cutoff = 3). The Wechsler Intelligence Scale was administered with a full-scale WISC-III of 66 (verbal IQ 73, performance IQ 67). She sometimes looked anxious, which manifested intermittently and briefly. Therefore, she was administered psychotropic drugs from 10 years of age. She had no histories of any other neurological illnesses including seizure and head injury. In addition, MRI examination revealed normal morphologies of the corpus callosum, anterior commissure, grey matter in anterior cingulate cortex, medial temporal lobe, olfactory bulb, pineal gland and cerebellum. The blood karyotype analysis result was also normal and "fragile X" was excluded. With respect to ocular phenotypes, the patient displayed reduced vision, photophobia and eyelid ptosis, but no other ocular abnormalities including aniridia. Her father carrying the same mutation did not show abnormal ocular phenotypes except for reduced vision and age-related macular degeneration (Fig. 3). Recently it is also known that PAX6 regulates proinsulin processing and glucose metabolism via modulation of PC1/3 production [37]. Therefore, we also checked blood glucose levels and BMIs (body mass indexes) of the patient and her father (the patient's BMI is 16.8 and her father's BMI is 22.4), and these measures were within normal limits.

Val46 is deemed to elicit functional impairment, because Leu46 is conserved from Drosophila to human (Fig. 1) and Leu46Arg and Leu46Pro mutations are reported to affect ocular phenotypes in previous studies [5,7]. Additionally, this mutation may be important for the following reasons: (1) the Leu46Val mutation is located in the paired domain, (2) structural analysis of this mutation using the Sequence Analysis Software "GENETYX" (GENETYX Co., Tokyo, Japan) suggests that it may disrupt the helix-turn-helix motif, and as a consequence the DNA-binding properties of the resulting mutated protein may vary, (3) this variant is predicted to be possibly damaging using a tool-website "PolyPhen" that can estimate the possible impact of an amino acid substitution on the structure and function of a protein (http://coot.embl.de/PolyPhen/), and (4) it is also possible that this mutation may exert its effect by disrupting the activity of an exonic splicing enhancer (ESE), because the SC35 score matrix of this mutation (3.17473) is lower than that of the wild type (4.09004), which is calculated using a tool-website "ESE finder" (an online resource to identify ESEs in query sequences) (http://rulai.cshl.edu/cgi-bin/tools/ESE3/esefinder.cgi?process=home). Therefore, these predicted functional consequences may be relevant to the autism phenotype, although the cosegregation was not observed in the present nuclear family.

A network of protein–protein interactions underlies complex biological processes. We addressed this issue using the Genome Network Platform (http://genomenetwork.nig.ac.jp/). There are 36 proteins that can interact with Pax6 and it is reported that 5 proteins out of the 36 proteins correlate with autism, which include HoxB1 [15,22], Tbp [6,31], Diaph1 [24,33], Ifi16 [1,11] and Ep300 [14,29] (Supplementary Fig. 1). For example, Hoxb1 that plays an important role in morphogenesis in all multicellular organisms can interact with both the paired domain and homeodomain of Pax6

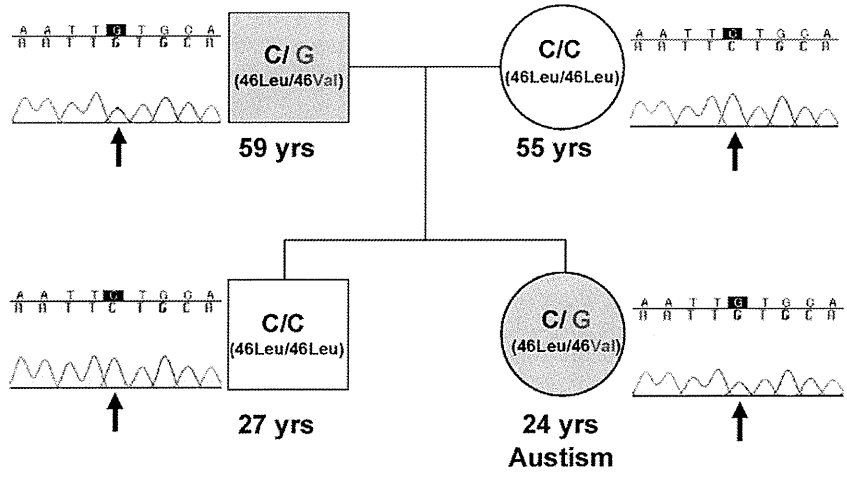

Fig. 2. Family structure of a patient with the *PAX6* missense mutation. Grey symbols indicate individuals carrying heterozygous *PAX6* Val46 allele. White symbols show the subjects with homozygous Leu46 alleles. Squares represent men and circles represent women. Genotype and sequence electrophelogram of each subject are also shown.

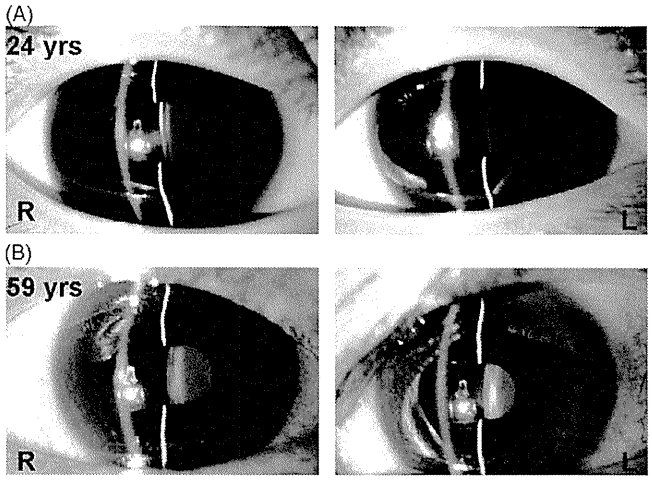

Fig. 3. Biomicroscopic observations of autistic patient (A) and her father (B) both of whom carry the mutant allele. (A) and (B) show the slit lamp aspects of ocular anterior segments as well as the lens of the subjects. Ages are also shown. R, right eye; L, left eye.

and can enhance Pax6-mediated transactivation of a minimal promoter that contains consensus Pax6 paired domain binding sites in *in vitro* experiments [22]. The Leu46Val missense mutation was located in the paired domain of PAX6. Therefore, the mutated PAX6 may affect the autism phenotype, owing to the attenuated interaction with HOXB1.

Concerning the penetrance of *PAX6* mutations in aniridia, it is known that *PAX6* missense mutations are a less frequent cause than expected [35], and they are not fully penetrant for other ocular anomalies [8]. Our current results that the Val46 allele did not cosegregate with autism or ocular phenotype in the family suggest that the Val46 of PAX6 may have only a modest effect, if any, on the development of autism and ocular abnormalities. It is also of note that in general autism is a multi-factorial disease caused by multiple susceptibility genes of small effect sizes, environmental factors and their interactions like other psychiatric illnesses [4].

MRI and functional MRI (fMRI) show that individuals with *PAX6* heterozygous mutations (haploinsufficiency) have structural abnormalities of grey matter in the anterior cingulated cortex, cerebellum and medial temporal lobe, as well as white matter deficits in the corpus callosum [9,10,13,23,30]. Additionally, patients of high-functioning autism with *PAX6* mutations (not haploinsufficiency) also have significant structural abnormalities [2,3,7]. In this study, we did not detect any abnormal brain structures in the patient. However, we previously reported that hippocampal neurogenesis is reduced in the *Pax6* heterozygous mutant rats that present behavioral abnormalities including decreased prepulse inhibition [18,19]. Therefore, we suspect that the autistic patient with the *PAX6* missense mutation may also have suffered from dampened hippocampal neurogenesis, potentially contributing to autism as one of the risk-conferring events [21].

In summary, we identified in this study a novel missense mutation of *PAX6* in one autistic patient with mild ocular abnormalities, and the mutation was not detected in 2120 nonautistic subjects. Further studies using larger samples and on the biological importance of this missense mutation are required.

Acknowledgements

We thank Dr. Yujiro Yoshihara for MRI inspection. We acknowledge the support of the Autism Genetics Resource Exchange (AGRE, http://www.agre.org) for the samples and thank the members of the Research Resource Center of the RIKEN Brain Science Institute for the sequencing and GeneScan genotyping services. This work was supported by RIKEN BSI Funds, grants from the Ministry of Education Culture, Sports, Science and Technology, the pharmacopsychiatry research grant from the Mitsubishi Pharma Research Foundation, a donation from the Maekawa Incorporated Medical Institution and CREST funds from the Japan Science and Technology Agency.

Appendix A. Supplementary data

Supplementary data associated with this article can be found, in the online version, at doi:10.1016/j.neulet.2009.07.021.

References

[1] B. Asefa, J.M. Dermott, P. Kaldis, K. Stefanisko, D.J. Garfinkel, J.R. Keller, p205, a potential tumor suppressor, inhibits cell proliferation via multiple pathways of cell cycle regulation, FEBS Lett. 580 (2006) 1205–1214.
[2] D.E. Bamiou, N.G. Campbell, F.E. Musiek, R. Taylor, W.K. Chong, A. Moore, V. van Heyningen, S. Free, S. Sisodiya, L.M. Luxon, Auditory and verbal working memory deficits in a child with congenital aniridia due to a PAX6 mutation, Int. J. Audiol. 46 (2007) 196–202.
[3] D.E. Bamiou, S.L. Free, S.M. Sisodiya, W.K. Chong, F. Musiek, K.A. Williamson, V. van Heyningen, A.T. Moore, D. Gadian, L.M. Luxon, Auditory interhemispheric transfer deficits, hearing difficulties, and brain magnetic resonance imaging abnormalities in children with congenital aniridia due to PAX6 mutations, Arch. Pediatr. Adolesc. Med. 161 (2007) 463–469.
[4] D.V. Bishop, Genes, cognition, and communication: insights from neurodevelopmental disorders, Ann. N. Y. Acad. Sci. 1156 (2009) 1–18.
[5] L.Y. Chao, R. Mishra, L.C. Strong, G.F. Saunders, Missense mutations in the DNA-binding region and termination codon in PAX6, Hum. Mutat. 21 (2003) 138–145.
[6] A. Cvekl, F. Kashanchi, J.N. Brady, J. Piatigorsky, Pax-6 interactions with TATA-box-binding protein and retinoblastoma protein, Invest. Ophthalmol. Vis. Sci. 40 (1999) 1343–1350.
[7] A. Dansault, G. David, C. Schwartz, C. Jaliffa, V. Vieira, G. de la Houssaye, K. Bigot, F. Catin, L. Tattu, C. Chopin, P. Halimi, O. Roche, N. Van Regemorter, F. Munier, D. Schorderet, J.L. Dufier, C. Marsac, D. Ricquier, M. Menasche, A. Penfornis, M. Abitbol, Three new PAX6 mutations including one causing an unusual ophthalmic phenotype associated with neurodevelopmental abnormalities, Mol. Vis. 13 (2007) 511–523.
[8] L.K. Davis, K.J. Meyer, D.S. Rudd, A.L. Librant, E.A. Epping, V.C. Sheffield, T.H. Wassink, Pax6 3′ deletion results in aniridia, autism and mental retardation, Hum. Genet. 123 (2008) 371–378.
[9] Z. Ellison-Wright, I. Heyman, I. Frampton, K. Rubia, X. Chitnis, I. Ellison-Wright, S.C. Williams, J. Suckling, A. Simmons, E. Bullmore, Heterozygous PAX6 mutation, adult brain structure and fronto-striato-thalamic function in a human family, Eur. J. Neurosci. 19 (2004) 1505–1512.
[10] G. Estivill-Torrus, T. Vitalis, P. Fernandez-Llebrez, D.J. Price, The transcription factor Pax6 is required for development of the diencephalic dorsal midline secretory radial glia that form the subcommissural organ, Mech. Dev. 109 (2001) 215–224.
[11] K. Garbett, P.J. Ebert, A. Mitchell, C. Lintas, B. Manzi, K. Mirnics, A.M. Persico, Immune transcriptome alterations in the temporal cortex of subjects with autism, Neurobiol. Dis. 30 (2008) 303–311.
[12] C. Graziano, A.V. D'Elia, L. Mazzanti, F. Moscano, S. Guidelli Guidi, E. Scarano, D. Turchetti, E. Franzoni, G. Romeo, G. Damante, M. Seri, A de novo nonsense mutation of PAX6 gene in a patient with aniridia, ataxia, and mental retardation, Am. J. Med. Genet. A 143A (2007) 1802–1805.
[13] I. Heyman, I. Frampton, V. van Heyningen, I. Hanson, P. Teague, A. Taylor, E. Simonoff, Psychiatric disorder and cognitive function in a family with an inherited novel mutation of the developmental control gene PAX6, Psychiatr. Genet. 9 (1999) 85–90.
[14] M.A. Hussain, J.F. Habener, Glucagon gene transcription activation mediated by synergistic interactions of pax-6 and cdx-2 with the p300 co-activator, J. Biol. Chem. 274 (1999) 28950–28957.
[15] J.L. Ingram, C.J. Stodgell, S.L. Hyman, D.A. Figlewicz, L.R. Weitkamp, P.M. Rodier, Discovery of allelic variants of HOXA1 and HOXB1: genetic susceptibility to autism spectrum disorders, Teratology 62 (2000) 393–405.
[16] Y. Iwayama, M. Maekawa, K. Yamada, T. Toyota, T. Ohnishi, Y. Iwata, K.J. Tsuchiya, G. Sugihara, M. Kikuchi, K. Hashimoto, M. Iyo, T. Inada, H. Kunugi, N. Ozaki, N. Iwata, S. Nanko, K. Iwamoto, Y. Okazaki, T. Kato, T. Yoshikawa, Association analyses between brain-expressed FABP (fatty-acid binding protein) genes and schizophrenia and bipolar disorder, Neuropsychiatr. Genet. (2009) Jun 24. [Epub].
[17] C. Lord, M. Rutter, A. Le Couteur, Autism diagnostic interview-revised: a revised version of a diagnostic interview for caregivers of individuals with possible pervasive developmental disorders, J. Autism Dev. Disord. 24 (1994) 659–685.
[18] M. Maekawa, N. Takashima, Y. Arai, T. Nomura, K. Inokuchi, S. Yuasa, N. Osumi, Pax6 is required for production and maintenance of progenitor cells in postnatal hippocampal neurogenesis, Genes Cells 10 (2005) 1001–1014.
[19] M. Maekawa, N. Takashima, M. Matsumata, S. Ikegami, M. Kontani, Y. Hara, H. Kawashima, Y. Owada, Y. Kiso, T. Yoshikawa, K. Inokuchi, N. Osumi, Arachi-